# Journal Pre-proof


Kinetics for the biodiesel production from lauric acid over Keggin heteropolyacid loaded in silica framework

Luis A. Gallego-Villada, Edwin A. Alarcón, Valeria Palermo, Patricia G. Vázquez, Gustavo P. Romanelli

PII: S1226-086X(20)30392-0

DOI: https://doi.org/10.1016/j.jiec.2020.08.030

Reference: JIEC 5198

To appear in: *Journal of Industrial and Engineering Chemistry*

Received Date: 26 June 2020

Revised Date: 25 August 2020

Accepted Date: 28 August 2020

Please cite this article as: Gallego-Villada LA, Alarcón EA, Palermo V, Vázquez PG, Romanelli GP, Kinetics for the biodiesel production from lauric acid over Keggin heteropolyacid loaded in silica framework, *Journal of Industrial and Engineering Chemistry* (2020), doi: https://doi.org/10.1016/j.jiec.2020.08.030

# Kinetics for the biodiesel production from lauric acid over Keggin heteropolyacid loaded in silica framework

Luis A. Gallego-Villada[a], Edwin A. Alarcón[a,*] edwin.alarcon@udea.edu.co, Valeria Palermo[b], Patricia G. Vázquez[b], and Gustavo P. Romanelli[b,c]

[a]Chemical Engineering Department, Environmental Catalysis Research Group, Universidad de Antioquia, Calle 70 N° 52-21, Medellín 050010, Colombia

[b]Centro de Investigación y Desarrollo en Ciencias Aplicadas "Dr. Jorge J. Ronco" CINDECA, (CONICET-CIC-UNLP), Facultad de Ciencias Exactas, Universidad Nacional de La Plata, Calle 47 Nº 257, B1900AJK, La Plata, Argentina.

[c]Cátedra de Química Orgánica, Facultad de Ciencias Agrarias y Forestales, Universidad Nacional de La Plata, Calles 60 y 119 s/n, B1904AAN, La Plata, Argentina.

[*] Corresponding author:
Edwin A. Alarcón, , +57 (4) 219 6609, Medellín 050010, Colombia

## Graphical Abstract

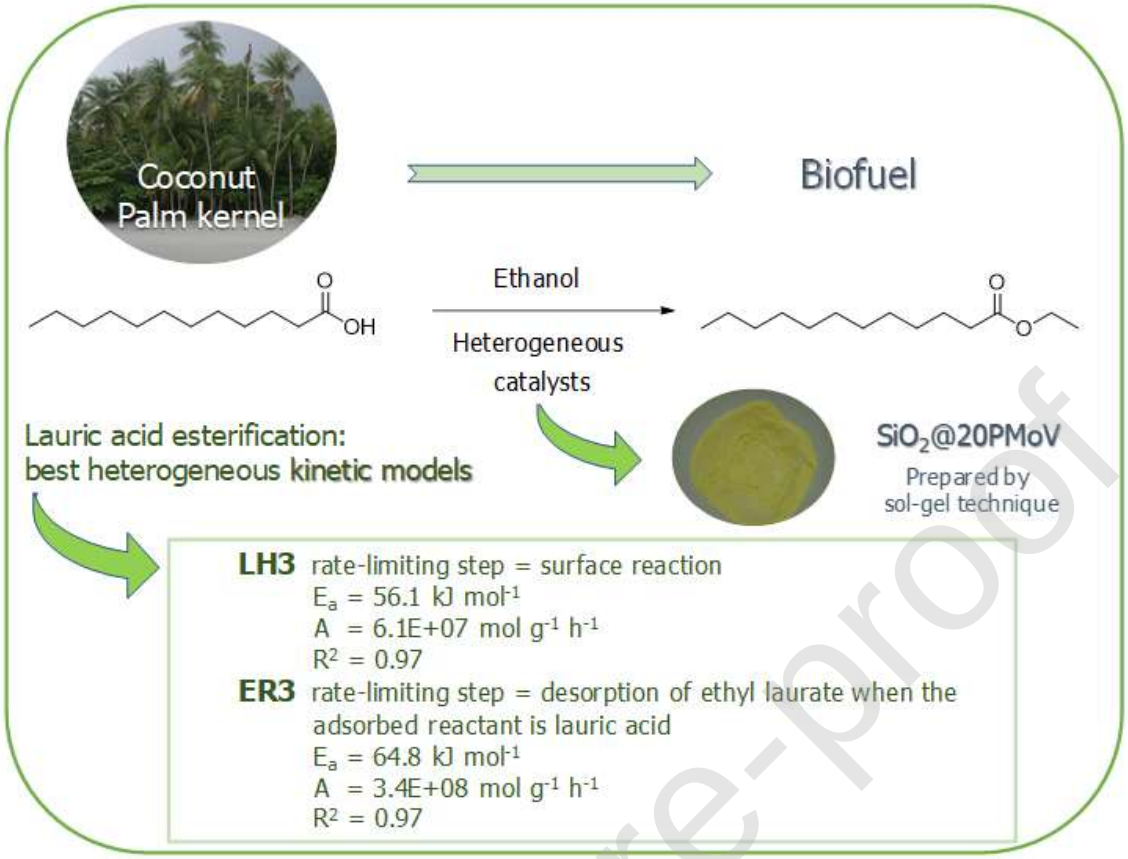


## Highlights

- $SiO_2$@20PMoV is highly active for lauric acid esterification with ethanol.
- $SiO_2$@20PMoV does not show loss of activity after 5 uses.
- The lauric acid esterification is described satisfactorily by LHHW or ER models.
- The activation energies were 56.1 kJ $mol^{-1}$ (LHHW) and 64.8 kJ $mol^{-1}$ (ER).

**Abstract**

Kinetic models were developed to describe the esterification reaction of lauric acid and ethanol over heterogeneous catalysts, which is a reaction of special interest in the biodiesel production. Vanadium Keggin heteropolyacid was included on a silica framework by sol-gel procedure, using different loadings. The synthesized materials were characterized by FT-IR, XRD, SEM, nitrogen adsorption/desorption isotherms, and

potentiometric titration, and tested as solid catalysts in the esterification of lauric acid. Best performance was achieved with $SiO_2$@20PMoV, which was used in the esterification of others fatty acid and alcohols. The reuse was successfully tested in five consecutive runs. Kinetic data using $SiO_2$@20PMoV were obtained at different temperatures (48 to 78 °C), fatty acid:alcohol molar ratios (4 mmol of lauric acid and 2.5, 5, 10 and 15 mL of ethanol), and catalyst amounts (12.5, 25 and 50 mg). The best heterogeneous models were LH3 (surface reaction as rate-limiting step) and ER3 (desorption of ethyl laurate as rate-limiting step when the adsorbed reactant is lauric acid). The activation energies were 56.1 kJ $mol^{-1}$ and 64.8 kJ $mol^{-1}$, and the reaction rate constants at 78 °C were 0.2791 mol $g^{-1}$ $h^{-1}$ and 0.0768 mol $g^{-1}$ $h^{-1}$ for LH3 and ER3, respectively.

***Keywords:*** Kinetic modeling, Esterification, Lauric acid, Heterogeneous catalysis, Biodiesel, Vanadium Keggin heteropolyacid.

## 1. Introduction

Biomass is a potential alternative to non-renewable fossil fuels for the future, due to aggravation of the energy crisis [1] and to that its use as feedstock reduces the $CO_2$ content in the atmosphere [2]. Biodiesel is a renewable fuel consist of long-chain esters formed from fatty acids and methanol or ethanol that can be obtained either by transesterification reaction of vegetable oils and fats or esterification reaction of fatty acids present in animal fats (e.g. lard or tallow) [3]; contrary to fossil-based diesel, biodiesel also offers biodegradability and non-toxicity [4]. The key factor of the globalization of biodiesel is its sustainability with available diesel engines without the need of mechanical modifications [5].

The esterification of carboxylic acids with alcohols or phenols is a useful preparation method of long-chain organic esters, which have many industrial applications, especially as biofuels [6]. Coconut and palm kernel oils are the major source of medium-chain fatty acids feedstocks, specifically with high content of lauric acid (dodecanoic acid, C12:0) [7,8]. Traditionally, esterification of fatty acid with alcohol is carried out over homogeneous mineral acid catalyst. Catalysts commonly used are: sulfuric acid, hydrochloric acid and organic acids like *p*-toluenesulfonic acid [9]. However, there are other types of the suitable catalysts for biodiesel synthesis as the heterogeneous or enzymatic catalysts, which offer easy separation of products and less wastewater, avoiding environmental issues and corrosion [10–12], and allowing continuous operating of reactors and catalyst reuse [13,14].

Different compounds have been tested as heterogeneous catalysts for biodiesel production: ionic exchange resins, supported-metal compounds, zeolites, and polymers are some representative examples [15–17]. In the last decades, heteropolyacids (HPAs)

have emerged as sustainable catalysts in Organic Chemistry due to these have been recognized as economically and environmentally benign acid catalysts due to their acidity and redox propertier for various reactions [18]. We have developed new materials based in them, for the use in the synthesis of heterocycles, eco-compatible oxidations with hydrogen peroxide, and recently in the valorization of biomass derivatives [19–22].

The major disadvantages of bulk HPAs derivatives are the low specific area (1-10 $m^2$ $g^{-1}$), low thermal stability and the high solubility in polar media [23]. For this reason and in order to overcome these problems, different supports were employed to immobilize HPAs, for example activated carbon, zeolites, silica, zirconium, titanium, MCM-41, and polymers among others [24,25]. Different HPAs in heterogeneous form have been tested in biodiesel production such as cesium-doped heteropoly tungstate (HPW), HPW/$ZrO_2$, HPW/$\gamma$-$Al_2O_3$ and HPW/$SiO_2$ for the simultaneous esterification and transesterification of 10% oleic acid-soybean oil mixture [26]; core-shell nanostructured heteropoly acid-functionalized zeolitic imidazolate frameworks-8 (ZIF-8) for rapeseed oil transesterification [18]; HPW/kaolinite, HPW/bentonite and HPW/montmorillonite for acetic acid esterification [27]; HPW/$SiO_2$ and cesium-doped HPW for rapeseed oil transesterification [28]; $H_3PMo_{12}O_{40}$/bentonite [29] for esterification of a waste from palm oil; $H_3PW_{12}O_{40}$/KIT-6 for neem oil transesterification [30]; 12-tungstophosphoric HPA/$ZrO_2$ [31], and $H_3PW_{12}O_{40}$ and $H_3PMo_{12}O_{40}$ supported on activated carbon fibers [32] for palmitic acid esterification; $Ni_{0.5}H_3SiW/SiO_2$ [33], NiHSiW/UiO-66 [34] and $Sn_{1.5}PW_{12}O_{40}$/Cu-BTC [35] for oleic acid esterification.

Pseudo-homogeneous kinetic models have been used to describe the biodiesel production from the lauric acid esterification with ethanol over several catalytic systems such as $ZnL_2$ [36], [(*n*-bu-$SO_3H$)MIM][$HSO_4$] [37], deep eutectic solvents based on cetyl

trimethyl ammonium bromide (CTAB) [38], and over 1-methyl-2-pyrrolidonium hydrogen sulfate ([Hnmp]$HSO_4$) [39] and silicotungstic acid encapsulated UiO-66 [40] using methanol. However, Langmuir-Hinshelwood-Hougen-Watson (LHHW) and Eley-Rideal (ER) heterogeneous kinetic models have been succesfully used to describe esterification kinetics of several heterogeneous catalytic systems for biodiesel production over niobium oxide [41], Amberlyst 46 [42], ion exchange resin [43], Amberlyst 15 [44] and 12-tungstophosphoric acid/SBA-15 [45]. Particularly for lauric acid esterification with ethanol, a heterogeneous kinetic study by Eley-Rideal mechanism over acid activated montmorillonite has been reported [46], which is a promising catalyst because of their low cost, thermal stability, reusability and mainly because their desirable catalytic properties such as high selectivity, high surface area, high pores dimension and presence of acid sites; furthermore, this catalyst allows to achieve a high equilibrium conversion around 90%. The experimental data of the heterogeneous reaction was successfully fitted to Eley-Rideal model with surface reaction between adsorbed ethanol and lauric acid as the rate-limiting step. A drawback of this study is the energy intensive in reaction due to the high temperature (180 °C); furthermore, the kinetic modeling using the LHHW mechanism-based models was not reported, which are typical kinetic models in biodiesel production over different heterogeneous catalytic as previously reported.

To date, there have been no reports on carrying out kinetic studies about esterification reaction for biodiesel production over vanadium Keggin heteropolyacids. Kinetic studies are receiving much importance since they provide the most powerful method of investigating the detailed reaction mechanisms, give information about the maximum product yield and specifically in the chemical industry, these kinetic models are the basis on which the modeling and the design of catalytic reactors is carried out as

well as the transition of production from molecular scale to macro scale [47], as is the case of biodiesel production, which has been one of the challenges worldwide in recent years. Thus, in this contribution, we successfully synthesized vanadium Keggin HPA included on a silica framework with different loads, which were tested as solid catalysts in the lauric acid esterification. The most important aim of this research is to develop a kinetic model to describe the esterification reaction for biodiesel production from lauric acid and ethanol on heterogeneous catalysts (Fig. 1).

Figure 1

## 2. Experimental

### 2.1. General

All reagents and solvents were of commercial analytical grade and used without further treatment, supplied by Sigma-Aldrich and Fluka.

### 2.2. Synthesis of Catalysts: PMoV Included on Silica

$H_4PMo_{11}VO_{40}$ (PMoV) was synthesized by a known hydrothermal procedure method described in the literature [48] (Supplementary Information).

This HPA was immobilized on silica containing four different loadings following a sol-gel procedure described in the literature with minor modifications [49]. A mixture of ethanol (2.95 mL), distilled water (9 mL), and a variable amount of PMoV (126, 252, 378, and 504 mg) was added to tetraethyl orthosilicate (11.2 mL), and stirred at 80 ºC, for 3 h, in a dry box in the absence of moisture. The hydrogel obtained was dehydrated at 80 ºC, for 2 h, in vacuum stove. The dried gel obtained was washed four times with ethanol at 78 ºC (3 x 10 mL) and dried at 80 ºC overnight. The prepared catalysts were named as

$SiO_2$@5PMoV, $SiO_2$@10PMoV, $SiO_2$@15PMoV, and $SiO_2$@20PMoV, where the numbers 5, 10, 15, and 20 indicate the percentage of PMoV load .

Also silica ($SiO_2$) was prepared following the same procedure, but using acetic acid instead of PMoV.

2.3. Catalyst Characterization

Fourier transform infrared spectra (FT-IR) of catalysts were acquired in the 400-4000 $cm^{-1}$ range using pellets with KBr in a Thermo Bruker IFS 66 FT-IR equipment.

X-ray diffraction (XRD) patterns were collected in Philips PW-1730 device, with Cu Kα radiation (λ= 1.5406 Å), 20 mA, 40 kV, and Ni filter. Scanning angle from 5° to 60° and scanning rate of 2° per minute were used.

Scanning electron microscopy (SEM) was recorded in a Philips 505 scanning electron microscope with an accelerating voltage of 25 eV. The solid samples were previously metallized with Au.

The specific surface area calculed by Brunauer–Emmett–Teller method, pore volume, and the mean pore diameter of the solids were determined by nitrogen adsorption/desorption isotherms at -196 °C in a Micromeritics ASAP 2020 equipment. The samples were previously degassed at 100 ºC for 12 h.

Potentiometric titration was used to determine the acidic properties of the catalysts, employing a 794 Basic Titrino Metrohm equipment and a double junction electrode. The solids were suspended in acetonitrile and titrated with *n*-butylamine in acetonitrile (0.025 N).

2.4. Catalytic Esterification Reaction

The selected reaction to evaluated the activity of the synthezised catalysts, was the esterification reaction of lauric acid with ethanol. In a test tube connected to a condenser, certain amount of lauric acid was added in a suspension of solid catalyst (of specific weight) in ethanol and the mixture was magnetically stirred for 24 h.

Three variables were analized: reaction temperature (48, 58, 68, and 78 °C); acid:alcohol molar ratio (4 mmol of lauric acid and 2.5, 5, 10 and 15 mL of ethanol), and catalyst amount (12.5, 25 and 50 mg). Samples were taken at regular intervals and the catalyst was removed by filtration. All experiments were repeated twice.

The progress of the reactions were quantified using calibration curve by GC/FID in a Shimadzu chromatograph model 2014, using a FID detector and a capillary column (SPB-1, length 30 m, I.D. 32 mm, and film thickness 1.00 μm). The carrier gas was high-purity nitrogen (≧99.999%), and the optimum conditions were as follows: splitless injection mode was used (1 μL), the injector temperature was set at 320 °C, the initial column temperature was 150 °C (held for 2 min), then ramped at 20°C/min to 200 °C.

To demonstrate the reusability of the prepared catalyst, it was separated by filtration after completion of the esterification reaction, washed twice with ethanol (1 mL), dried in a vacuum oven at 20 °C for 24 h, and reused in a five successive runs under the same conditions.

After the optimization of reaction conditions, the esterification was extended to others fatty acids and alcohols. The products were identified by GC–MS Mass Spectrometry using a HP 5971 mass detector coupled to a HP gas chromatograph (Supplementary Information).

2.5. Kinetic Modeling

For the kinetic analysis of the esterification reaction (Eq. 1) of lauric acid with ethanol, kinetic data were carried out at different temperatures (48-78 °C), ethanol amounts (2.5-15 mL), catalyst amounts (12.5-50 mg) and ten reaction times varying from 0.5 until 24 h. These data were used to test several proposed kinetic models, which are described below. The experimental conditions studied in this work are presented in Table 1.

$$A + B \leftrightarrow C + D \quad (1)$$

Where A is the fatty acid (lauric acid, $C_{12}H_{24}O_2$), B is the alcohol (ethanol, $C_2H_5OH$), C is the ethyl ester (ethyl laurate, $C_{14}H_{28}O_2$) and D is water ($H_2O$).

Table 1

*2.5.1. Pseudo-Homogeneous Reversible Model*

A homogeneous-like model [6,36,41] was tested using the experimental data, for the purpose of evaluating a possible simplification of the heterogeneous kinetics adapted to homogeneous model. The rate law (Eq. (2)) of lauric acid can be written as:

$$\frac{dC_A}{dt} = r_A = \frac{W}{V_{rxn}}\left(-k_1 {C_A}^{\alpha} {C_B}^{\beta} + k_2 {C_C}^{\gamma} {C_D}^{\delta}\right) \quad (2)$$

Where $C_i$ is the molar concentration of specie i, t is reaction time, W is the weight of catalyst, $V_{rxn}$ is the reaction volume, $r_A$ is the formation reaction rate of lauric acid, $k_1$ and $k_2$ are the direct and reverse reaction constants, respectively. α, β, γ and δ are the reaction orders respect to lauric acid, ethanol, ethyl laurate and water, respectively.

Molar concentrations are related to the conversion (X) of lauric acid by Eq. (3), where $C_{i0}$ is the initial concentration of specie i, $\theta_i$ is defined by Eq. (4), and $\gamma_i$ is the stoichiometric coefficient of the specie i in esterification reaction and it is positive for products and negative for reactants.

$$C_i = C_{A0}(\theta_i + \gamma_i X) \tag{3}$$

$$\theta_i = \frac{C_{i0}}{C_{A0}} \tag{4}$$

The Arrhenius' equation was used to calculated the kinetic constants considering the direct ($k_1$) and reversible ($k_2$) reaction equations (Eq. (5)), as follows:

$$k_i = A_i exp\left(-\frac{Ea_i}{RT}\right) \tag{5}$$

Where $A_i$ is the pre-exponential factor of reaction i, $Ea_i$ is the activation energy of reaction i, R is the ideal gas constant and T is the temperature.

Finally, Eq. (6) is obtained by replacing Eqs. (3) – (5) in Eq. (2).

$$\frac{dX}{dt} = \frac{W}{V_{rxn}}\left(A_1 exp\left(-\frac{Ea_1}{RT}\right) {C_{A0}}^{\alpha+\beta-1}(1-X)^{\alpha}(\theta_B - X)^{\beta} - A_2 exp\left(-\frac{Ea_2}{RT}\right) {C_{A0}}^{\gamma+\delta-1} X^{\gamma+\delta}\right) \tag{6}$$

The objective function (OF) presented in Eq. (7) was minimized for finding the optimal parameters $A_1$, $A_2$, $Ea_1$, $Ea_2$, α, β, γ, δ; it was done using the *fmincon* subroutine from Matlab®.

$$OF = \sum_{i}^{N_t}\left({X_i}^{Exp} - {X_i}^{Mod}\right)^2 \tag{7}$$

$X_i^{Exp}$ and $X_i^{Mod}$ are the experimental and model values of lauric acid conversion and $N_t$ is related to experimental set. It is worth to mention that the kinetic parameters were

obtained from a global estimation by regressing of experimental kinetic data for all conditions presented in Table 1.

*2.5.2. Heterogeneous Models*

Several heterogeneous models were proposed to evaluate them in the kinetics of the esterification reaction of lauric acid with ethanol. A total of 17 models were tested, which 5 of them correspond to Langmuir-Hinshelwood-Hougen-Watson (LHHW) kinetic models (Table 2) and 12 to Eley-Rideal (ER) kinetic models (Table 3). All of them assume that diffusion steps were not rate-limiting and that reactants do not dissociate [41]; in addition, they consider reversible reactions, products are not present in the beginning of the reaction and either surface reaction, adsorption or desorption as the rate-limiting step. LHHW models consider that both reactants are adsorbed while ER models consider that only one reactant is adsorbed, while the other is in the liquid phase [41]. The derivation of equations for each model considering different rate-limiting steps for determination of esterification reaction rate constants is given in Supplementary Information, Appendix A is for LHHW models and Appendix B is for ER models.

Table 2

Table 3

The reaction rate is related with lauric acid conversion (X) according to Eq. (8) [42]:

$$r = -r_A = \frac{V_{rxn} C_{A0}}{W} \frac{dX}{dt} = \frac{N_{A0}}{W} \frac{dX}{dt} \rightarrow \frac{dX}{dt} = \frac{W}{N_{A0}} r \quad (8)$$

Where $-r_A$ is the lauric acid reaction rate and it is equal to expressions given by Tables 2 and 3 for rate equation (r), W is the weight of catalyst, $V_{rxn}$ is the reaction volume, $C_{A0}$ is the initial concentration of lauric acid, $N_{A0}$ are the initial moles of lauric acid, t is reaction time, $C_i$ is the molar concentration of specie i (Eq. (3)), $k_i$ are the reaction constants and $K_i$ are the equilibrium constants.

The Arrhenius' equation (Eq. (5)) was used to calculated the kinetic constants (k). Temperature dependence of $K_i$ is known from the chemical reaction isotherm equation (Van't Hoff equation) and the definition of Gibbs free energy ($\Delta G°$), which is given in Eq. (9) [43,50,51]. It is assumed that the reaction enthalpy ($\Delta H°$) and reaction entropy ($\Delta S°$) are both constants within the experimental temperature range [43].

$$K_i = \frac{k_i}{k_{-i}} = exp\left(\frac{-\Delta G°}{RT}\right) = exp\left(\frac{\Delta S°}{R}\right) exp\left(\frac{-\Delta H°}{RT}\right) \quad (9)$$

Where $k_i$ and $k_{-i}$ is the constant of direct and reverse reaction, respectively. As ($-\Delta S°$) is considered constant, the Eq. (9) is simplified to Eq. (10), which it is similar form to Arrhenius law. This is the mathematical expression used in this work for the equilibrium constants of adsorption, surface reaction and desorption.

$$K_i = A_i exp\left(\frac{-\Delta H°}{RT}\right) \quad (10)$$

The objective function (OF) presented in Eq. (7) was minimized for finding the optimal parameters for each one of the heterogeneous models of Tables 2 and 3; it was done using the *fmincon* subroutine from Matlab®. For each model, the root mean square error (RMSE), normalized root mean square error (NRMSE) and determination coefficient ($R^2$) were calculated by Eqs. (11-13), respectively [44].

$$RMSE = \sqrt{\frac{\sum_i^{N_t}\left(X_i^{Exp} - X_i^{Mod}\right)^2}{N_t}} \quad (11)$$

$$NRMSE = \frac{RMSE}{\max(x_i) - \min(x_i)} \quad (12)$$

$$R^2 = 1 - \frac{\sum_i^{N_t}\left(X_i^{Exp} - X_i^{Mod}\right)^2}{\sum_i^{N_t}\left(X_i^{Exp} - \bar{X}^{Exp}\right)^2} \quad (13)$$

Where $N_t$ is the total data points used for calculation, $\max(x_i)$ and $\min(x_i)$ is the largest and smallest value, respectively, for lauric acid conversion in experimental data set, and $\bar{X}^{Exp}$ is the mean of experimental data.

## 3. Results and Discussion

### 3.1. Catalyts Characterization

FT-IR spectra of the synthesized catalysts are similar to the pure silica. They present signals which are associated to amorphous silica: 3500 $cm^{-1}$ (δSi-OH), 1639 $cm^{-1}$ (δO-H), 1080 $cm^{-1}$ (νO-Si-O), 951 $cm^{-1}$ (νSi-OH), 797 $cm^{-1}$, and 453 $cm^{-1}$ (δO-Si-O) [49] which mask the characteristic peaks of Keggin structure of PMoV (1060 $cm^{-1}$ (νP-Oa), 960 $cm^{-1}$ (νMo-Od), 864 $cm^{-1}$ (νMo-Ob-Mo), 777 $cm^{-1}$ (νMo-Oc-Mo)) [52]. Fig. 2 shows an interval of the spectra of PMoV, $SiO_2$, and the representative catalyst $SiO_2$@20PMoV.

Figure 2

Fig. 3 shows the X-ray diffraction patterns of PMoV, $SiO_2$, and $SiO_2$@20PMoV. The bulk PMoV pattern presents the distinctive signals of Keggin structure in the intervals 2θ = 6-10º, 16-23º, and 25-36º [53], although these peaks are not present in the included

catalysts since are masked by the large diffraction peak of the amorphous silica patterns. $SiO_2$@20PMoV presents the same driffraction shape of an amorphous material [54].

Figure 3

The amorphous nature of the silica [55], with the typical laminar morphology and size irregularity are observeed in the SEM micrographs for $SiO_2$ and $SiO_2$@20PMoV, without porosity in the 500x magnification (Fig. 4). The similitude in the FT-IR spectra, XRD patterns and SEM images among of include catalysts and silica, indicates that the PMoV is well disperse into the silica framework.

Figure 4

The nitrogen adsorption/desorption isotherms of the included catalysts are typical Langmuir isotherms [56], which indicate that the synthezised solid are microporous materials (Fig. S1-S5, Supplementary Information). Specific surface area ($S_{BET}$), pore volume and pore size distribution of silica and catalysts are presented in Table 4. It can be seen that the values of included catalysts are similar to pure silica. Lower values are obtained for $SiO_2$@5PMoV and $SiO_2$@10PMoV, which can be attributed to pore blocking by the remaining PMoV inside silica framework. On the other hand, with an increase of PMoV load, the strong compression during sol-gel process is prevent by the PMoV excess, resulting in an increment in the superficial area, pore volume and size.

Table 4

The curves acquired by potentiometric titration with *n*-butylamine, allow obtain the maximum acid strength of the surface sites and the total number of acid sites. The former is indicated by the initial potential ($E_0$) and the total number of acid sites is given by the plateau. The acid strength of catalysts are listed in Table 4. The incorporation of PMoV into the silica framework produce a $E_0$ decreament, because the protons can interact with $SiO_2$. The acid strength of included catalysts increases with the PMoV load increment. Pure silica and $SiO_2$@5PMoV has strong sites ($100 > E_0 > 0$ mV) meanwhile the other catalysts have very strong acid sites ($E_0 > 100$ mV), according to Cid and Pecchi clasification [57]. This characteristic allow the use of this materials as acid catalysts in the esterification of lauric acid. Fig. 5 shows the PMoV, $SiO_2$@20PMoV, and $SiO_2$ titration curves.

Figure 5

3.2. Catalytic Esterification Reaction

*3.2.1. Effect of Heteropoly Acid Amount*

The effect of the HPA amount in the catalyst has been studied in the esterification reaction of lauric acid with ethanol at 58 °C, using 4 mmol of fatty acid, 10 mL of alcohol and 25 mg of catalyst. Fig. 6 shows the conversion profile of lauric acid for different PMoV loadings and the respective blank, that is, without catalyst. It is observed that the fatty acid conversion at specific time increases as the HPA loading increases from 0 to 15%; however, using more than 15% does not significantly affect the conversion.

Figure 6

*3.2.2. Catalyst Reuse*

The reusability of heterogeneous catalyst is one of its main advantages compared to homogeneous catalysts. This characteristic has been studied in the esterification reaction of lauric acid with ethanol at 58 °C by running consecutive reaction cycles under the same reaction conditions, using 4 mmol of fatty acid, 10 mL of alcohol and 25 mg of catalyst with a heteropoly acid loading of 20% ($SiO_2$@20PMoV). Fig. 7 shows that the lauric acid conversion during five cycles is very similar, indicating the high stability of the heterogeneous catalyst.

Figure 7

*3.2.3. Effect of Chain Length on Esterification Reaction*

The effect of the fatty acid has been studied in the esterification reaction with ethanol at 78 °C by 5 h, using 4 mmol of fatty acid, 10 mL of alcohol and 25 mg of $SiO_2$@20PMoV. Fig. 8 shows the effect of different fatty acids. Under the same reaction conditions, the conversion of fatty acid decreases as the length of the fatty acid chain increases, obtaining the highest conversion (98%) with lauric acid and the lowest conversion with stearic (18:0) and oleic (18:1) acids, whose values are 83% and 80%, respectively. This behavior has been evidenced previously for the esterification reaction of oleic and acetic acid with ethanol, using Amberlyst 15 as a catalyst [44].

Figure 8

*3.2.4. Effect of Alcohol*

The effect of the alcohol nature has been studied in the esterification reaction with lauric acid at 78 °C by 5 h, using 4 mmol of fatty acid, 10 mL of alcohol and 25 mg $SiO_2$@20PMoV. Fig. 9 shows that lauric acid conversion is strongly dependent to the alcohol nature. It is observed that higher conversion is achieved, in general, for the longer linear chain alcohols such as isopentanol, *n*-butanol, *n*-propanol and ethanol. By comparison the phenol and the benzyl alcohol, it is concluded that the location of the hydroxyl group has a very important effect, because the lauric acid conversion is less when phenol is used probably due to the aromatic nature of carbon. In addition, a significant steric effect on the tertiary carbon has been reported in the literature for the esterification of stearic acid with 1- and 2-butanol at 150 °C, using a montmorillonite-based clay catalyst [58]. The above can be checked with the results obtained for butanol isomers, since the lauric acid conversion is 98%, 90% and 44% for *n*-butanol, *s*-butanol and *ter*-butanol, respectively, corresponding to a primary, secondary, and tertiary alcohol, respectively. Similar conclusions are obtained for *i*-propanol and *n*-propanol. An important difference is observed between the conversion with methanol and ethanol, which can be justified by their boiling point, whose values are approximately 64.7 °C and 78.4 °C, respectively, which implies that methanol evaporates at the reaction temperature and there is not enough alcohol in the reaction mixture for the reaction to be carried out properly.

Figure 9

*3.2.5. Effect of Catalyst Amount*

The effect of the catalyst amount, with $SiO_2$@20PMoV, has been studied in the esterification reaction of lauric acid with ethanol at 58 °C, using 4 mmol of fatty acid and 10 mL of alcohol. Fig. 10 shows that the lauric acid conversion at specific time increases as the catalyst amount increases from 12.5 to 50 mg, indicating the great importance of catalyst surface availability for esters formation.

*3.2.6. Effect of Ethanol Amount*

The effect of the ethanol amount has been studied in the esterification reaction of lauric acid with ethanol at 58 °C, using 4 mmol of fatty acid and 25 mg of catalyst ($SiO_2$@20PMoV). Fig. 11 shows that the lauric acid conversion is not significantly different, at a specific time, for the four ethanol to lauric acid molar ratios studied. This probably occurs because the molar ratios correspond to values between 10.7 and 64.2, which are well above the values reported in literature [44] as 1, 3, and 5, using acetic and oleic acid with ethanol, which indicates that there is a large excess of alcohol in the reaction. For other reaction systems, the esterification increased as the ethanol to fatty acid ratio increased, indicating that ethanol facilitates fatty acid conversion on the surface of the catalyst during the reaction [44].

*3.2.7. Effect of Temperature*

The effect of temperature has been studied in the esterification reaction of lauric acid with ethanol, using 4 mmol of fatty acid, 10 mL of alcohol and 25 mg of catalyst ($SiO_2$@20PMoV). Fig. 12 shows that the lauric acid conversion, at a specific time,

increases when the reaction temperature is increased from 48 to 78 °C. Conversions around 100% are reached at 24 h with all temperatures, except for 48 °C, which reaches about 60%.

## 3.3. Kinetic Modeling

### *3.3.1. Pseudo-Homogeneous Model*

The optimal values for kinetic parameters of pseudo-homogeneous model described by Eq. (6) are reported in Table 5 with the corresponding determination coefficient ($R^2$) of the model, which corresponds to 85.79%. Some heterogeneous kinetic models are studied below, which is coherent due to the catalyst used in this work. Fig. S6-S8 (Supplementary Information) show graphically the behavior of the pseugo-homogeneous model with respect to the experimental data.

Table 5

The activation energies calculated by pseudo-homogeneous model, for this esterification reaction catalyzed by different catalysts are shown in Table 6. The catalyst studied in this work showed $E_a$ for direct reaction lower than $ZnL_2$ and $[Hnmp]HSO_4$ but higher values than the other catalysts for both direct and reverse reaction. However, the results are biased by the not so good fit of this model ($R^2$ = 85.79%). More reliable results are shown below for heterogeneous models.

Table 6

*3.3.2. Heterogeneous Models*

Table 7 present the results of LHHW and ER kinetic model fitting analysis. These results were obtained assuming that equilibrium constants are constant in the temperature range studied (48-78 °C), which can be a good estimation and approximation (based on [43]) for finding the kinetic parameters through non-linear regression, because there is a large parameters set. The best LHHW model to describe the esterification reaction of lauric acid with ethanol with the heterogeneous catalyst was, slightly better, LH3, followed by LH2, because LH3 shows the best statistical parameters, highest $R^2$ (94.7%) and lowest RMSE (0.065) and NRMSE (0.065). This means that using LHHW kinetic model, the limiting step of the esterification is the surface reaction as has been reported in the literature for oleic acid esterification with ethanol catalyzed by Amberlyst 15 as catalyst [44] or acetic acid esterification with isopropyl alcohol catalyzed by ion exchange resin [43].

Table 7

Based on the statistical parameters as mentioned above, the best ER models to describe the esterification reaction of lauric acid were ER3 and ER6, which corresponds to desorption of ethyl laurate or water as rate-limiting step, respectively, when the adsorbed reactant is lauric acid. These models are so similar due to rate equation expressions are similar because it was assumed that there were initially none of the products. In conclusion, model fitting for lauric acid esterification indicates that the ER model describes the reaction slightly better than LHHW model, when the equilibrium constants are considered constant in temperature range.

The two previous models (LH3 and ER3) were taken, one for each type of kinetic model, to determine the kinetic parameters considering the variation of the equilibrium constants with temperature (Eq. (10)). The parameters are shown in Table 8, where the fitting for the LH3 model ($R^2$ = 96.7%) is improved compared to corresponding shown in Table 7 considering $K_i$ constants ($R^2$ = 94.7%). However, for the ER3 model, the improvement is very slight since $R^2$ is 96.7% instead of 96.0%. Due to the adsorption is an exothermic process and desorption an endothermic process [59], the enthalpy changes are negative and positive, respectively, as shown in Table 8. The energy activation values do not change significantly between the LH3 and ER3 models in Tables 7 and 8.

Table 8

The lauric acid esterification with ethanol can be described by either the LH3 or ER3 models, taking into account the dependence of equilibrium constants with the temperature. Both models show a higher fitting to experimental data in comparison with pseudo-homogeneous model. Fig. 10-12 show graphically the behavior of LH3 and ER3 models with respect to the experimental data.

Figure 10

Figure 11

Figure 12

The active sites correspond to Brönsted acid sites associated with available hydrogen on the Keggin structure. These structures are within the pores or on the surface of silica support through its interaction with silanols. The presence of Brönsted acid sites have been demonstrated by pyridine-FTIR in the commercial Keggin HPAs with similar structure [60]. The LHHW (LH3) and the Eley-Rideal (ER3) mechanism-based models were proposed as potential reaction mechanisms for esterification of lauric acid with ethanol over Keggin heteropolyacid loaded in silica framework. The following reaction steps were proposed, where S represents the surface site on catalyst.

- **LH3 (surface reaction as the rate limiting-step)**

$$A + S \underset{k_{-A}}{\overset{k_A}{\leftrightarrow}} A.S \quad \text{adsorption of lauric acid} \tag{14a}$$

$$B + S \underset{k_{-B}}{\overset{k_B}{\leftrightarrow}} B.S \quad \text{adsorption of ethanol} \tag{14b}$$

$$A.S + B.S \underset{k_{-S}}{\overset{k_S}{\leftrightarrow}} C.S + D.S \quad \text{surface reaction} \tag{14c}$$

$$C.S \underset{k_{-C}}{\overset{k_C}{\leftrightarrow}} C + S \quad \text{desorption of ethyl laurate} \tag{14d}$$

$$D.S \underset{k_{-D}}{\overset{k_D}{\leftrightarrow}} D + S \quad \text{desorption of water} \tag{14e}$$

- **ER3 (ethyl laurate desorption as the rate limiting-step)**

$$A + S \underset{k_{-A}}{\overset{k_A}{\leftrightarrow}} A.S \quad \text{adsorption of lauric acid} \tag{15a}$$

$$A.S + B \underset{k_{-S}}{\overset{k_S}{\leftrightarrow}} C.S + D \quad \text{surface reaction} \tag{15b}$$

$$C.S \underset{k_{-C}}{\overset{k_C}{\leftrightarrow}} C + S \quad \text{desorption of ethyl laurate} \tag{15c}$$

The above mechanism-based models are in accordance with reported for other esterification reactions such as the lauric acid esterification with ethanol over acid activated montmorillonite [46], the oleic acid esterification with methanol over Amberlyst 46 [42], the esterification reaction of acetic and oleic acids with ethanol over Amberlyst 15 [44] and the lauric acid esterification with glycerol over 12-tungstophosphoric acid/SBA-15 [45].

## 4. Conclusions

Kinetic models were developed to describe the esterification reaction of lauric acid and ethanol on heterogeneous catalysts vanadium Keggin HPA included on a silica framework. This reaction has special interes in the biodiesel production. Four catalysts with different PMoV loadings were synthesized by sol-gel procedure, charactherized and tested as solid catalysts in the esterification of lauric acid. Best catalytic performance was achieved with $SiO_2$@20PMoV, and its reusability was successfully proven in five consecutive runs. Moreover, the esterification was extended to others fatty acids and alcohols. Kinetic data with $SiO_2$@20PMoV catalyst were recolected at different temperatures, acid:alcohol molar ratios, and catalyst amounts, and used in a pseudo-homogeneous reversible model and LHHW and ER heterogeneous models. LH3 was the best LHHW model, with the surface reaction as the rate-limiting step of the lauric acid esterification, while ER3 was the best ER model, which corresponds to desorption of ethyl laurate as the rate-limiting step when the adsorbed reactant is lauric acid. The LH3 and ER3 heterogeneous models showed a higher fitting to experimental data than pseudo-

homogeneous model ($R^2$ = 96.7% for both models greather than 85.8%), whose activation energies were 56.1 kJ $mol^{-1}$ and 64.8 kJ $mol^{-1}$, pre-exponential factors were 6.1E+07 and 3.4E+08 mol $g^{-1}$ $h^{-1}$, and the reaction rate constants at 78 °C were 0.2791 mol $g^{-1}$ $h^{-1}$ and 0.0768 mol $g^{-1}$ $h^{-1}$ for LH3 and ER3, respectively.

**Declaration of interests**

The authors declare that they have no known competing financial interests or personal relationships that could have appeared to influence the work reported in this paper.

## Acknowledgments

The authors thank to G. Valle, J. Tara, and M. Theiller, for the experimental measurements. We also thank to UNLP, CONICET, and ERANET for the financial support. VP, PGV, and GPR are members of CONICET.

## References

[1] X. Tang, S. Niu, S. Zhao, X. Zhang, X. Li, H. Yu, C. Lu, K. Han, J. Ind. Eng. Chem. 77 (2019) 432–40. 10.1016/j.jiec.2019.05.008.

[2] G.D. Yadav, A.R. Yadav, Chem. Eng. J. 243 (2014) 556–63. 10.1016/j.cej.2014.01.013.

[3] X.-X. Han, K.-K. Chen, W. Yan, C.-T. Hung, L.-L. Liu, P.-H. Wu, K.-C. Lin, S.-B. Liu, Fuel 165 (2016) 115–22. 10.1016/j.fuel.2015.10.027.

[4] X. Tang, S. Niu, J. Ind. Eng. Chem. 69 (2019) 187–95. 10.1016/j.jiec.2018.09.016.

[5] S.Y. Chua, L.A. Periasamy, C.M.H. Goh, Y.H. Tan, N.M. Mubarak, J. Kansedo, M. Khalid, R. Walvekar, E.C. Abdullah, J. Ind. Eng. Chem. 81 (2020) 41–60. 10.1016/j.jiec.2019.09.022.

[6] M. Banchero, G. Gozzelino, Energies 11(7) (2018) 1843. 10.3390/en11071843.

[7] F.D. Gunstone, J.L. Harwood, A.J. Dijkstra, The Lipid Handbook, 3rd ed., Boca Raton, London: CRC Press, 2007.

[8] D.C. Taylor, M.A. Smith, P. Fobert, E. Mietkiewska, R.J. Weselake, Comprehensive Biotechnology, Vol. 4, 2nd ed., Elsevier, 2011, pp. 67–85.

[9] S. Ganesan, S. Nadarajah, M. Khairuddean, G.B. Teh, Renew. Energy 140 (2019)

9–16. 10.1016/j.renene.2019.03.031.

[10] A. Gaurav, S. Dumas, C.T.Q. Mai, F.T.T. Ng, Green Energy Environ. 4(3) (2019) 328–41. 10.1016/j.gee.2019.03.004.

[11] S. Furuta, H. Matsuhashi, K. Arata, Catal. Commun. 5(12) (2004) 721–3. 10.1016/j.catcom.2004.09.001.

[12] J. Boro, A.J. Thakur, D. Deka, Fuel Process. Technol. 92(10) (2011) 2061–7. 10.1016/j.fuproc.2011.06.008.

[13] N.A. Abas, R. Yusoff, M.K. Aroua, H. Abdul Aziz, Z. Idris, Chem. Eng. J. 382 (2020) 122975. 10.1016/j.cej.2019.122975.

[14] A.I. Tropecêlo, M.H. Casimiro, I.M. Fonseca, A.M. Ramos, J. Vital, J.E. Castanheiro, Appl. Catal. A Gen. 390(1–2) (2010) 183–9. 10.1016/j.apcata.2010.10.007.

[15] R. Gomes Prado, M.L. Bianchi, E. Gaspar da Mota, S. Silva Brum, J. Henrique Lopes, M.J. da Silva, Waste and Biomass Valorization 9(4) (2018) 669–79. 10.1007/s12649-017-0012-0.

[16] M.A. Hanif, S. Nisar, U. Rashid, Catal. Rev. 59(2) (2017) 165–88. 10.1080/01614940.2017.1321452.

[17] K. Vasić, G. Hojnik Podrepšek, Ž. Knez, M. Leitgeb, Catalysts 10(2) (2020) 237. 10.3390/catal10020237.

[18] Y. Jeon, W.S. Chi, J. Hwang, D.H. Kim, J.H. Kim, Y.-G. Shul, Appl. Catal. B Environ. 242 (2019) 51–9. 10.1016/j.apcatb.2018.09.071.

[19] L.M. Sanchez, H.J. Thomas, M.J. Climent, G.P. Romanelli, S. Iborra, Catal. Rev. - Sci. Eng. 58(4) (2016) 497–586. 10.1080/01614940.2016.1248721.

[20] O.M. Portilla-Zuñiga, Á.G. Sathicq, J.J. Martínez, S.A. Fernandes, T.R.M. Rezende, G.P. Romanelli, Sustain. Chem. Pharm. 10(257) (2018) 50–5. 10.1016/j.scp.2018.09.002.

[21] M. Palacio, P.I. Villabrille, V. Palermo, G.P. Romanelli, J. Sol-Gel Sci. Technol. 95 (2020) 321–31. 10.1007/s10971-020-05239-6.

[22] D.M. Morales, R.A. Frenzel, G.P. Romanelli, L.R. Pizzio, Mol. Catal. 481 (2020) 110210. 10.1016/j.mcat.2018.10.005.

[23] H. Rastegari, H.S. Ghaziaskar, J. Ind. Eng. Chem. 21 (2015) 856–61. 10.1016/j.jiec.2014.04.023.

[24] O.D.S. Lacerda, R.M. Cavalcanti, T.M. De Matos, R.S. Angélica, G.N. Da Rocha Filho, I.D.C. Lopes Barros, Fuel 108 (2013) 604–11. 10.1016/j.fuel.2013.01.008.

[25] V. Şimşek, K. Mürtezaoğlu, Bilecik Şeyh Edebali Üniversitesi Fen Bilim. Derg. 6(1) (2019) 91–103. 10.35193/bseufbd.553967.

[26] R. Sheikh, M. Choi, J. Im, Y. Park, J. Ind. Eng. Chem. 19(4) (2013) 1413–9. 10.1016/j.jiec.2013.01.005.

[27] A. Alsalme, A.A. Alsharif, H. Al-Enizi, M. Khan, S.G. Alshammari, M.A. Alotaibi, R.A. Khan, M.R.H. Siddiqui, J. Chem. 2018 (2018) 1–10. 10.1155/2018/7037461.

[28] B. Hamad, R.O. Lopes de Souza, G. Sapaly, M.G. Carneiro Rocha, P.G. Pries de Oliveira, W.A. Gonzalez, E. Andrade Sales, N. Essayem, Catal. Commun. 10(1) (2008) 92–7. 10.1016/j.catcom.2008.07.040.

[29] A. de N. de Oliveira, M.A. Barbosa de Lima, L.H. de Oliveira Pires, M. Rosas da Silva, P.T. Souza da Luz, R.S. Angélica, G.N. da Rocha Filho, C.E. F. da Costa, R. Luque, L.A. Santos do Nascimento, Materials (Basel). 12(9) (2019) 1431. 10.3390/ma12091431.

[30] P. Sudhakar, A. Pandurangan, Mater. Renew. Sustain. Energy 8(4) (2019) 22. 10.1007/s40243-019-0160-1.

[31] J. Alcañiz-Monge, B. El Bakkali, G. Trautwein, S. Reinoso, Appl. Catal. B Environ. 224 (2018) 194–203. 10.1016/j.apcatb.2017.10.066.

[32] J. Alcañiz-Monge, G. Trautwein, J.P. Marco-Lozar, Appl. Catal. A Gen. 468 (2013) 432–41. 10.1016/j.apcata.2013.09.006.

[33] Q. Zhang, D. Lei, Q. Luo, T. Deng, J. Cheng, Y. Zhang, P. Ma, Period. Polytech. Chem. Eng. (Ii) (2019) 1–7. 10.3311/PPch.14788.

[34] Q. Zhang, D. Ling, D. Lei, T. Deng, Y. Zhang, P. Ma, Green Process. Synth. 9(1) (2020) 131–8. 10.1515/gps-2020-0014.

[35] Q. Zhang, D. Ling, D. Lei, J. Wang, X. Liu, Y. Zhang, P. Ma, Front. Chem. 8(March) (2020) 1–10. 10.3389/fchem.2020.00129.

[36] E.J.M. De Paiva, V. Graeser, F. Wypych, M.L. Corazza, Fuel 117(Part A) (2014) 125–32. 10.1016/j.fuel.2013.09.016.

[37] Z. Wei, F. Li, H. Xing, S. Deng, Q. Ren, Korean J. Chem. Eng. 26(3) (2009) 666–72. 10.1007/s11814-009-0111-0.

[38] K. Li, X. Chen, W. Xue, Z. Zeng, S. Jiang, Int. J. Chem. Kinet. 51(5) (2019) 329–36. 10.1002/kin.21256.

[39] B. Han, W. Zhang, F. Yin, S. Liu, X. Zhao, J. Liu, C. Wang, H. Yang, R. Soc. Open Sci. 5(9) (2018) 180672. 10.1098/rsos.180672.

[40] Q. Zhang, T. Yang, X. Liu, C. Yue, L. Ao, T. Deng, Y. Zhang, RSC Adv. 9(29) (2019) 16357–65. 10.1039/C9RA03209F.

[41] J. De Araújo Gonaçalves, A.L.D. Ramos, L.L.L. Rocha, A.K. Domingos, R.S. Monteiro, J.S. Peres, N.C. Furtado, C.A. Taft, D.A.G. Aranda, J. Phys. Org. Chem. 24(1) (2011) 54–64. 10.1002/poc.1701.

[42] O. Ilgen, Fuel Process. Technol. 124 (2014) 134–9. 10.1016/j.fuproc.2014.02.023.

[43] Y. Liu, J. Liu, H. Yan, Z. Zhou, A. Zhou, ACS Omega 4 (2019) 19462–8. 10.1021/acsomega.9b02994.

[44] A. Shahid, Y. Jamal, S.J. Khan, J.A. Khan, B. Boulanger, Arab. J. Sci. Eng. 43(11) (2018) 5701–9. 10.1007/s13369-017-2927-y.

[45] P. Hoo, A.Z. Abdullah, Ind. Eng. Chem. Res. 54(32) (2015) 7852–8. 10.1021/acs.iecr.5b02304.

[46] P.R.S. Dos Santos, F. Wypych, F.A.P. Voll, F. Hamerski, M.L. Corazza, Fuel 181(x) (2016) 600–9. 10.1016/j.fuel.2016.05.026.

[47] L.A. Petrov, Y. Alhamed, A. Al-Zahrani, M. Daous, Chinese J. Catal. 32(6–8) (2011) 1085–112. 10.1016/S1872-2067(10)60225-2.

[48] F. Kern, S. Ruf, G. Emig, Appl. Catal. A Gen. 150(1) (1997) 143–51. 10.1016/S0926-860X 96 00286-4.

[49] V. Palermo, Á. Sathicq, T. Constantieux, J. Rodríguez, P. Vázquez, G. Romanelli, Catal. Letters 145(4) (2015) 1022–32. 10.1007/s10562-015-1498-3.

[50] Chemistry LibreTexts, The Van't Hoff Equation. Available at: https://chem.libretexts.org/. Accessed January 11, 2020.

[51] L.E. Revell, B.E. Williamson, J. Chem. Educ. 90(8) (2013) 1024–7. 10.1021/ed400086w.

[52] L.R. Pizzio, P.G. Vázquez, C.V. Cáceres, M.N. Blanco, Appl. Catal. A Gen. 256(1–2) (2003) 125–39. 10.1016/S0926-860X(03)00394-6.

[53] A. Popa, V. Sasca, E.E. Kiss, R. Marinkovic-Neducin, M.T. Bokorov, I. Holclajtner-Antunović, Mater. Chem. Phys. 119(3) (2010) 465–70. 10.1016/j.matchemphys.2009.09.026.

[54] J.R. Martínez, S. Palomares-Sánchez, G. Ortega-Zarzosa, F. Ruiz, Y. Chumakov, Mater. Lett. 60(29–30) (2006) 3526–9. 10.1016/j.matlet.2006.03.044.

[55] E. Papirer, Adsorption on Silica Surfaces, Marcel Dekker, New York, 2000.

[56] J.D. Wright, N.A.J.M. Sommerdijk, Sol-Gel Materials Chemistry and Applications. Taylor & Francis Group, Boca Raton, 2001.

[57] R. Cid, G. Pecchi, Appl. Catal. 14 (1985) 15–21. 10.1016/S0166-9834(00)84340-7.

[58] S. Bouguerra Neji, M. Trabelsi, M. Frikha, Energies 2(4) (2009) 1107–17. 10.3390/en20401107.

[59] H. Lynggaard, A. Andreasen, C. Stegelmann, P. Stoltze, 77 (2004) 71–137. 10.1016/j.progsurf.2004.09.001.

[60] Y. Yang, G. Lv, W. Guo, L. Zhang, Microporous Mesoporous Mater. 261 (2018) 214–9. 10.1016/j.micromeso.2017.11.018.

**Fig. 1.** Scheme of lauric acid esterification with ethanol.

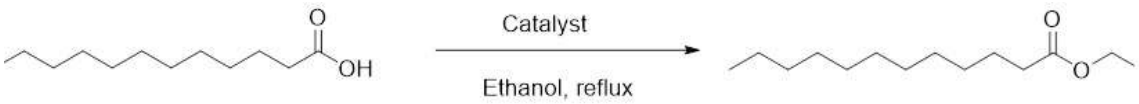


**Fig. 2.** FT-IR spectra of PMoV, $SiO_2$@20PMoV, and $SiO_2$.

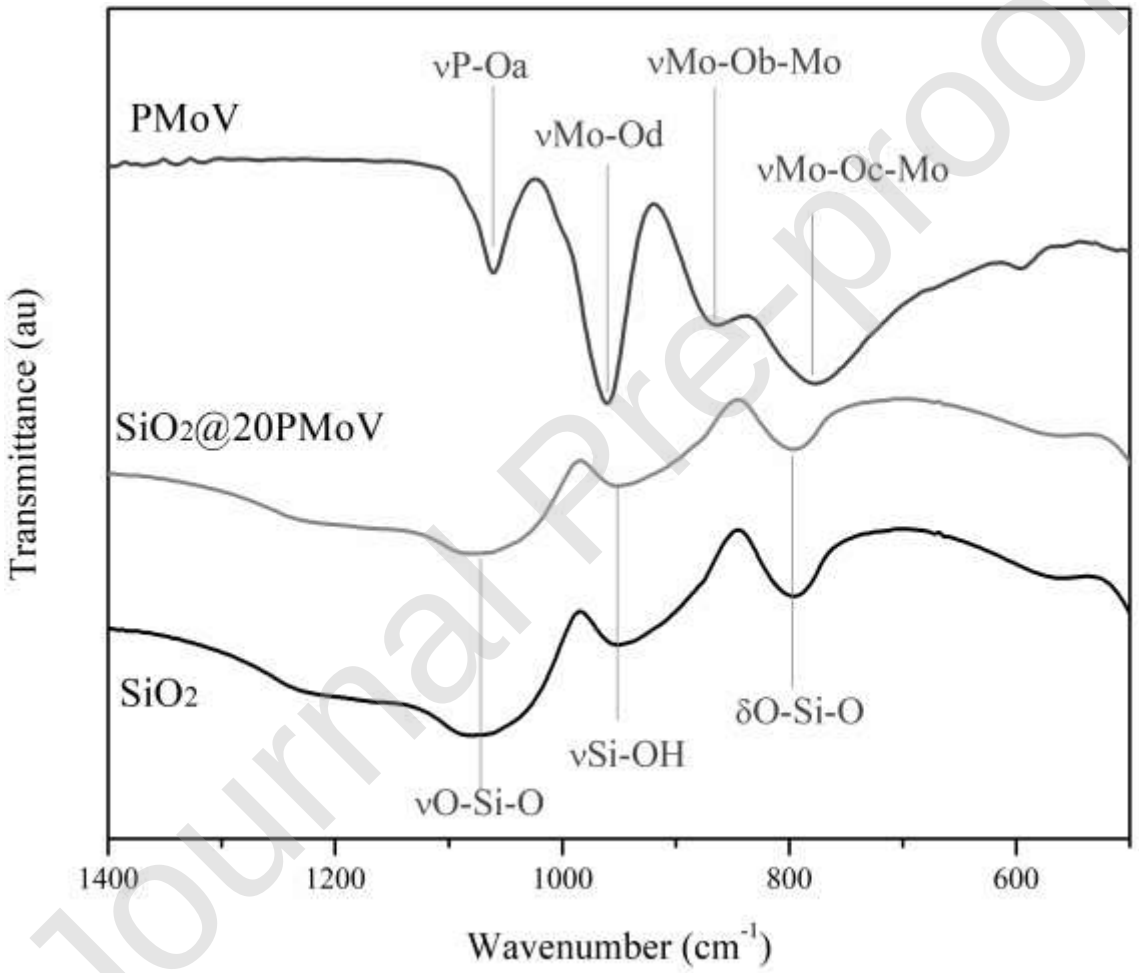


**Fig. 3.** XRD patterns of PMoV, $SiO_2$@20PMoV, and $SiO_2$.

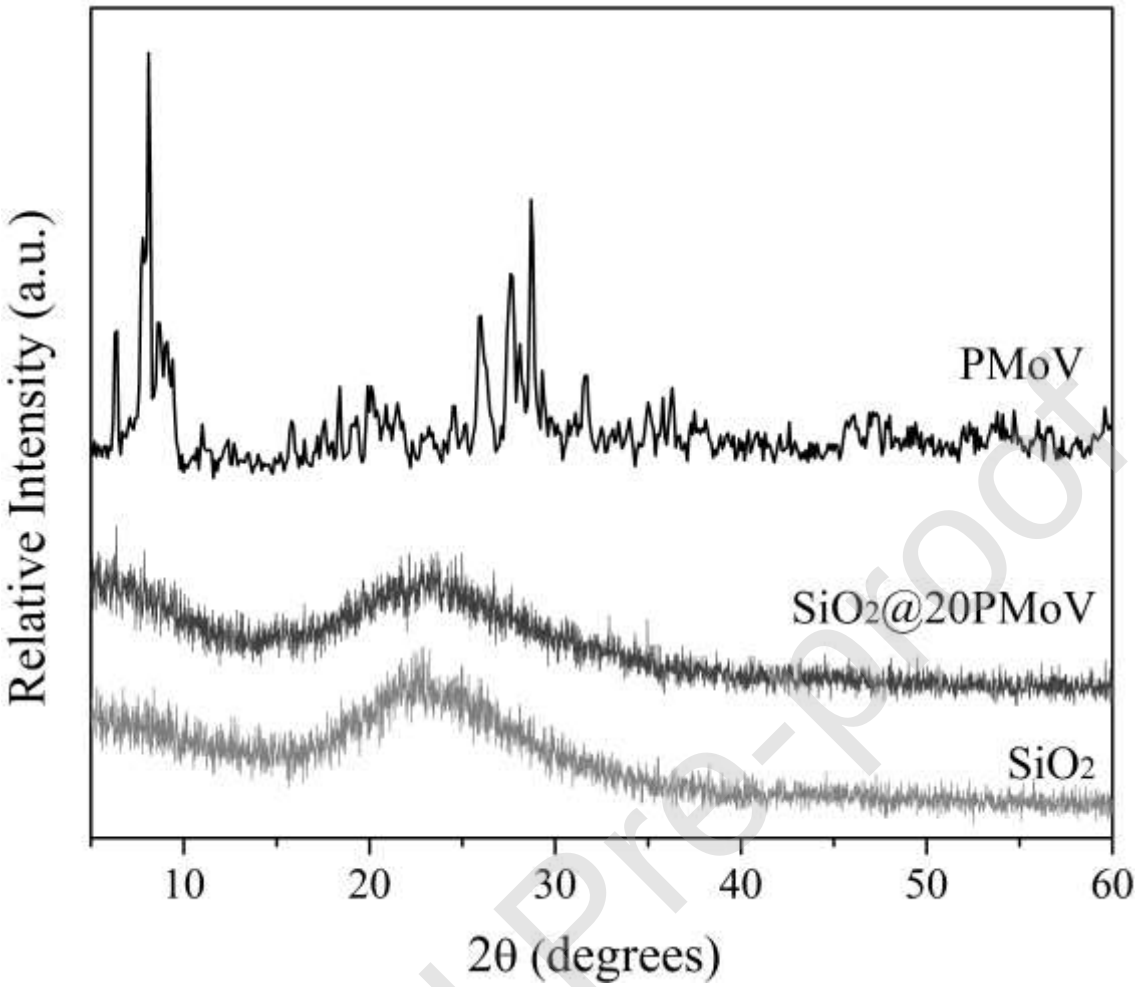


**Fig. 4.** SEM x500 micrographs of $SiO_2$@20PMoV (left) and $SiO_2$ (right).

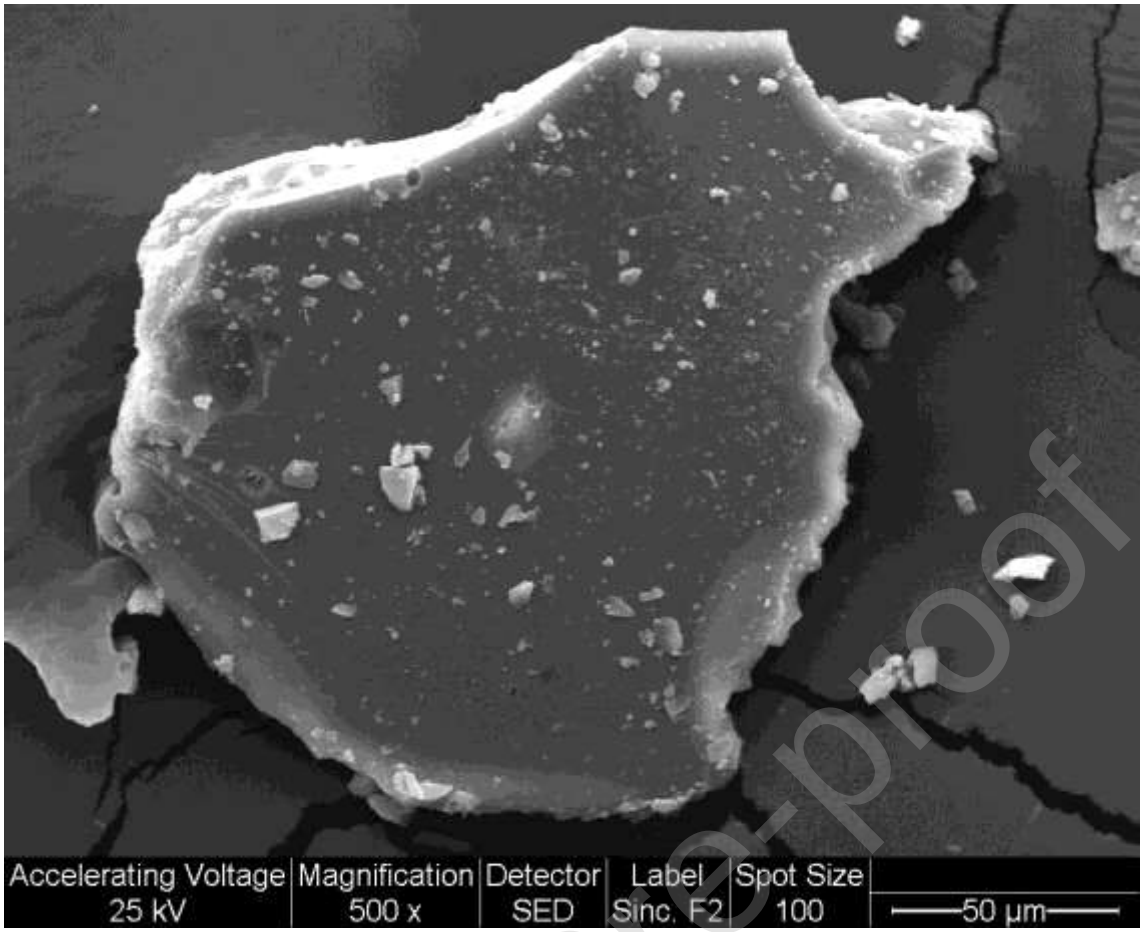

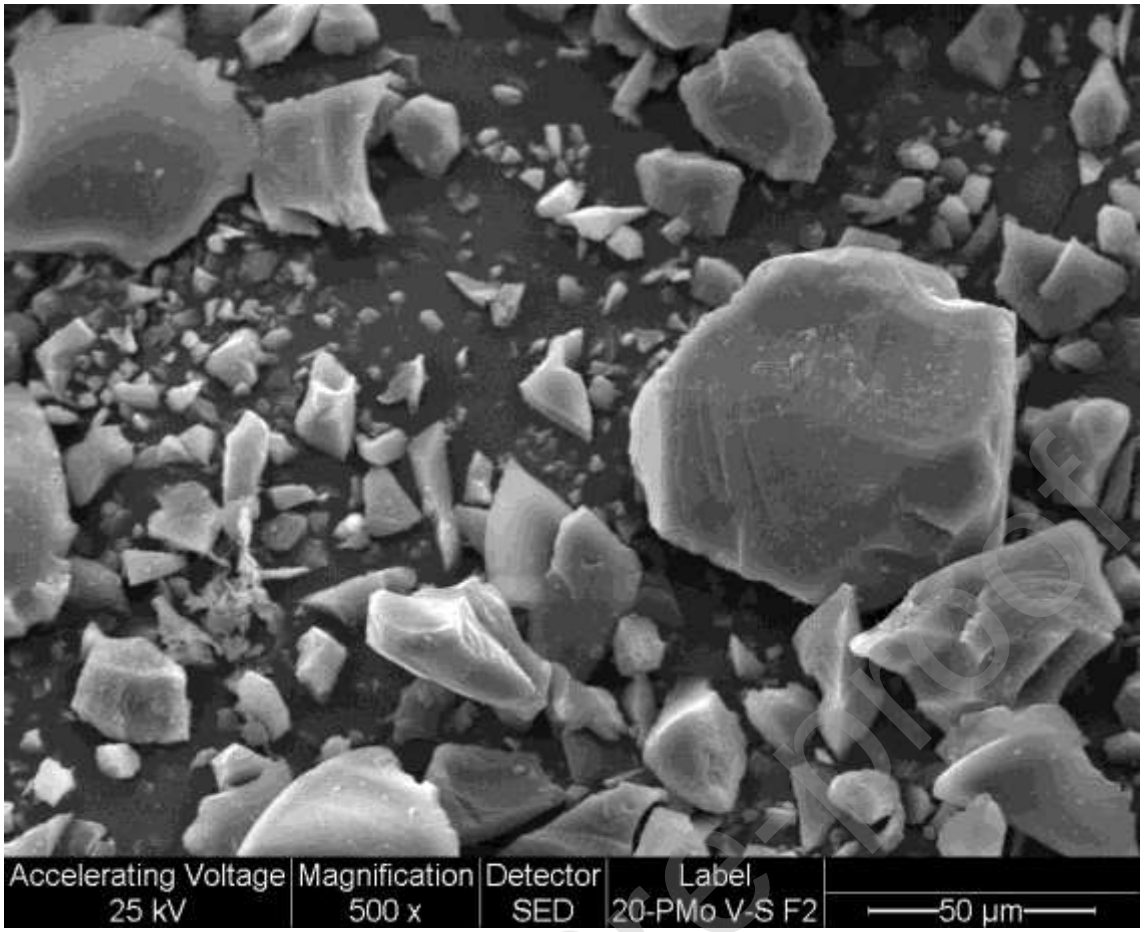


**Fig. 5.** Potentiometric titration with n-butylamine of PMoV, $SiO_2$@20PMoV, and $SiO_2$.

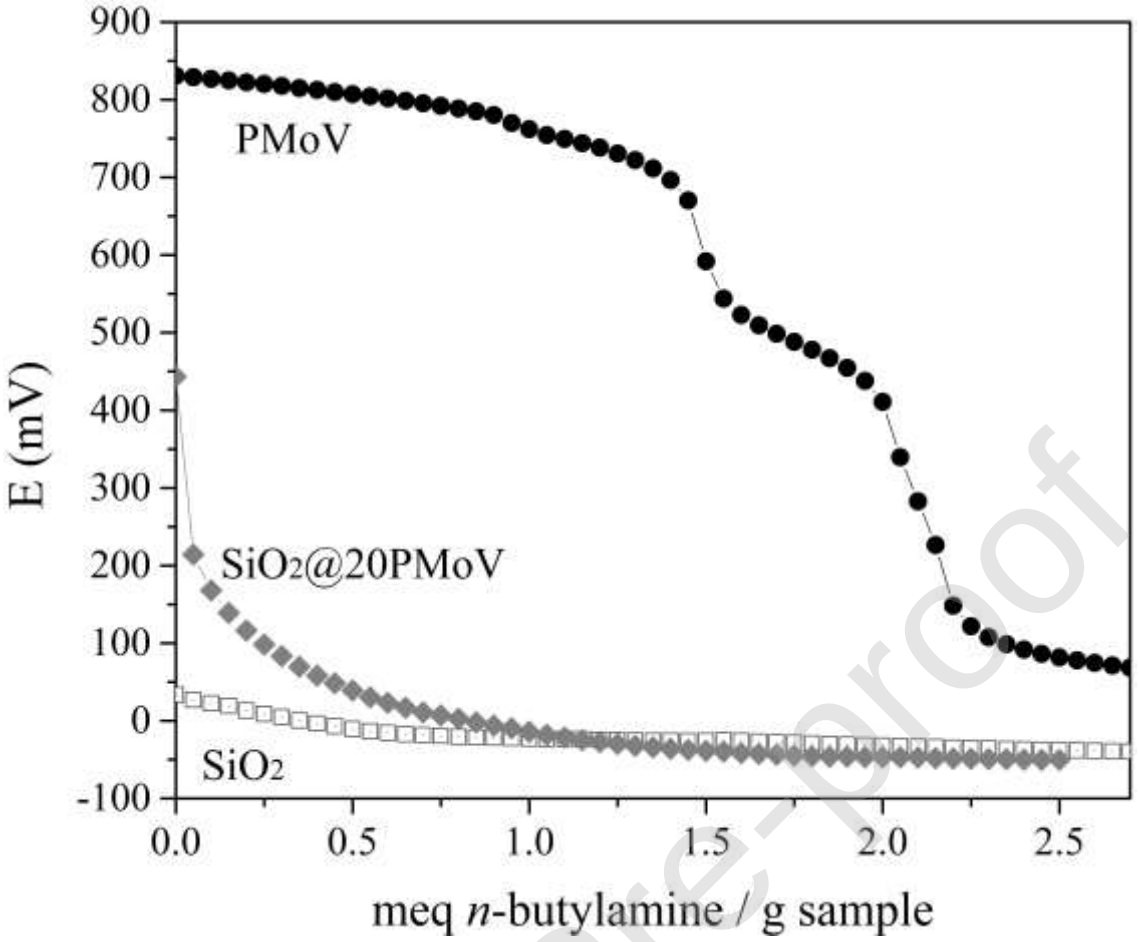


**Fig. 6.** Effect of HPA loading in conversion profile of lauric acid in esterification reaction. Reaction conditions: 4 mmol lauric acid, 10 mL ethanol, 25 mg catalyst, 58 °C.

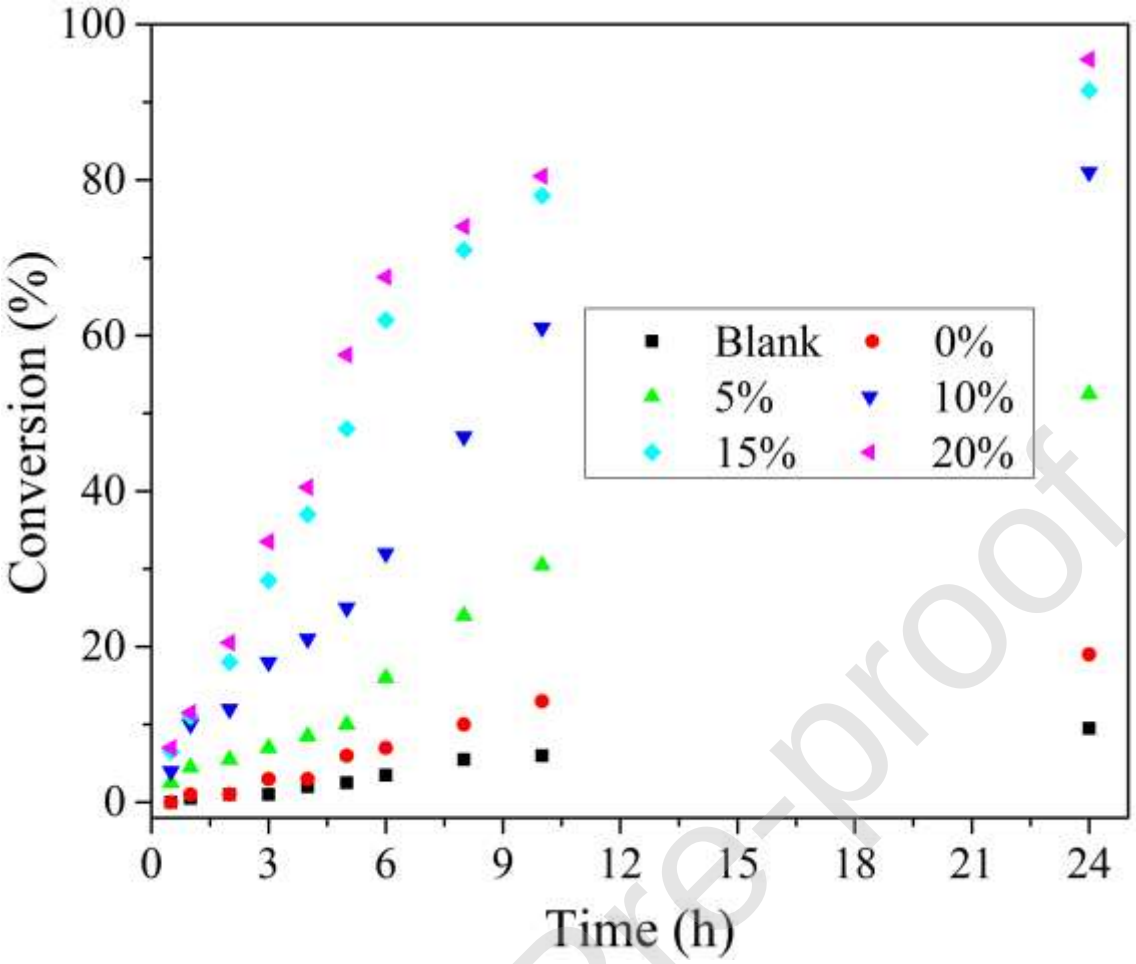


**Fig. 7.** Catalytic activity in the esterification reaction of lauric acid with ethanol, in five consecutive cycles. Reaction conditions: 4 mmol lauric acid, 10 mL ethanol, 25 mg $SiO_2$@20PMoV, 58 °C.

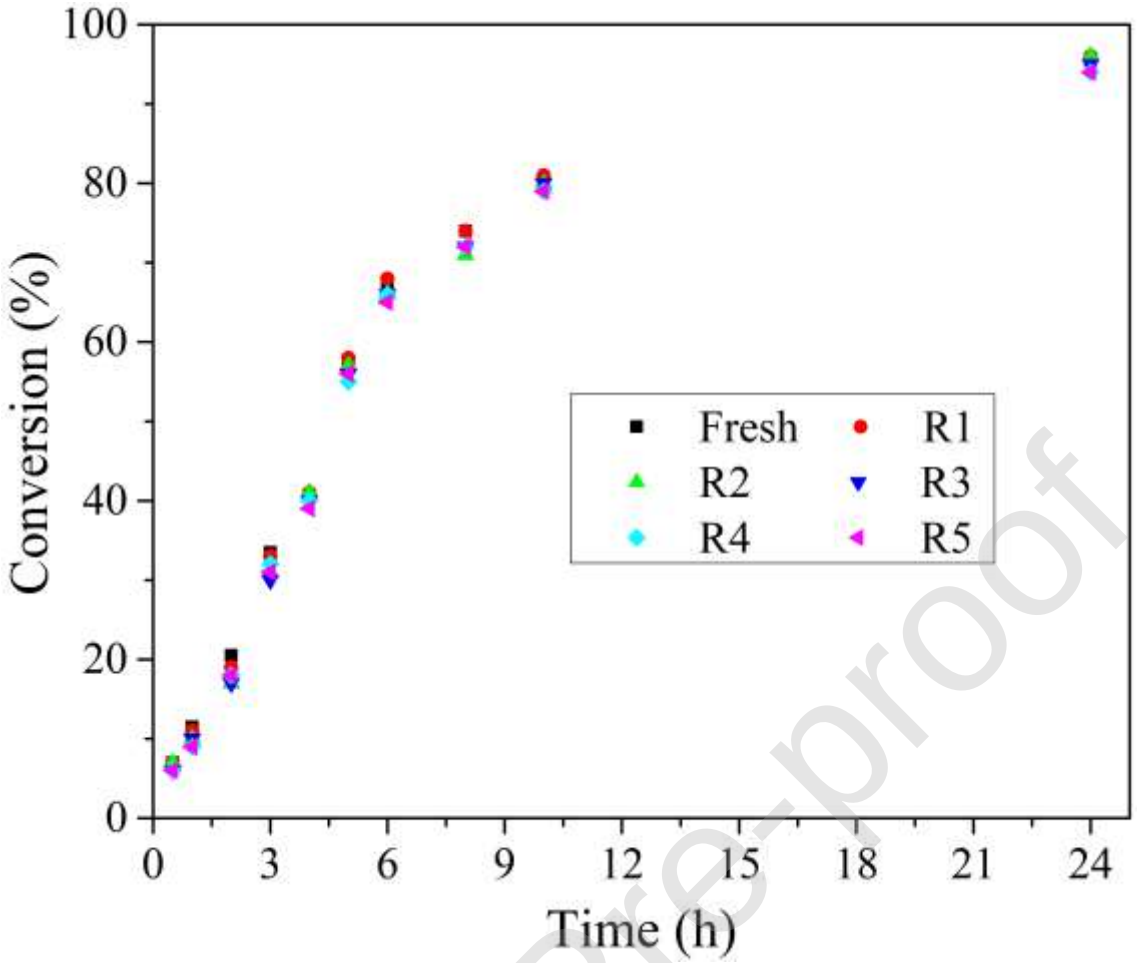


**Fig. 8.** Effect of fatty acid in conversion at 5 h in esterification reaction. Reaction conditions: 4 mmol fatty acid, 10 mL ethanol, 25 mg $SiO_2$@20PMoV, 78 °C.

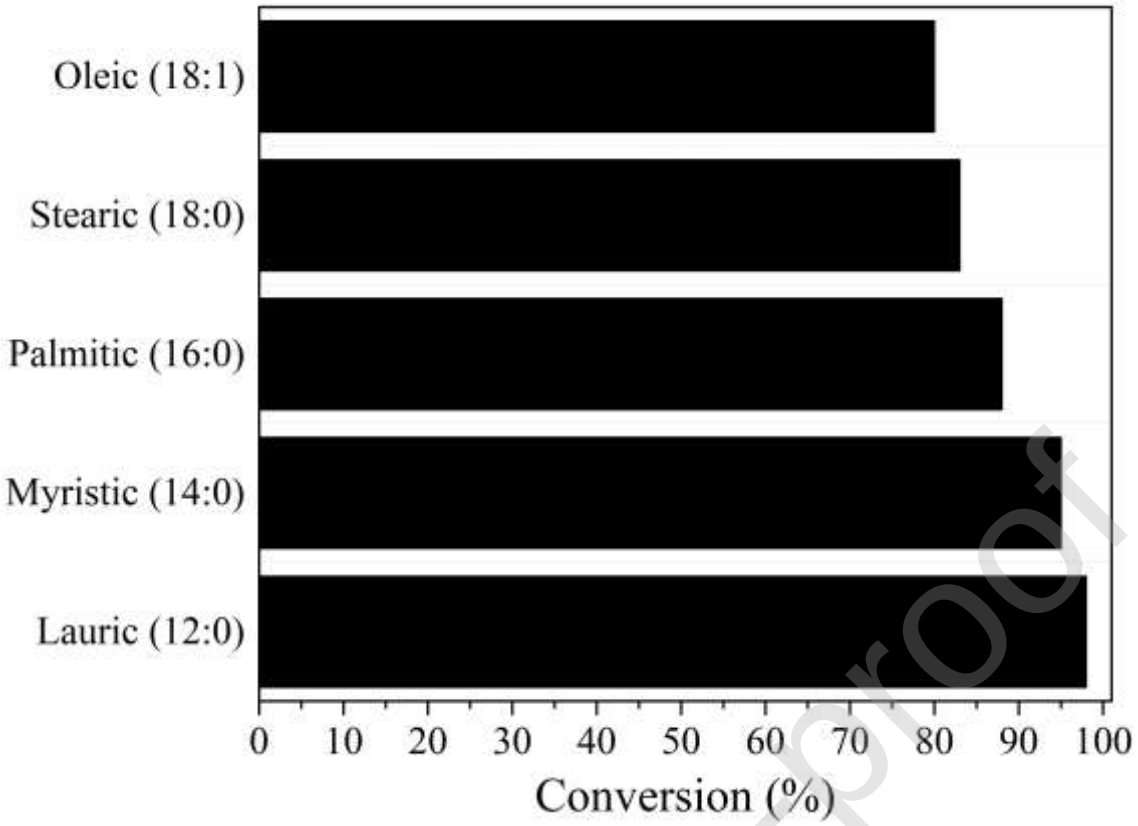


**Fig. 9.** Effect of alcohol nature in conversion of lauric acid at 5 h in esterification reaction. Reaction conditions: 4 mmol lauric acid, 10 mL alcohol, 25 mg $SiO_2$@20PMoV, 78 °C.

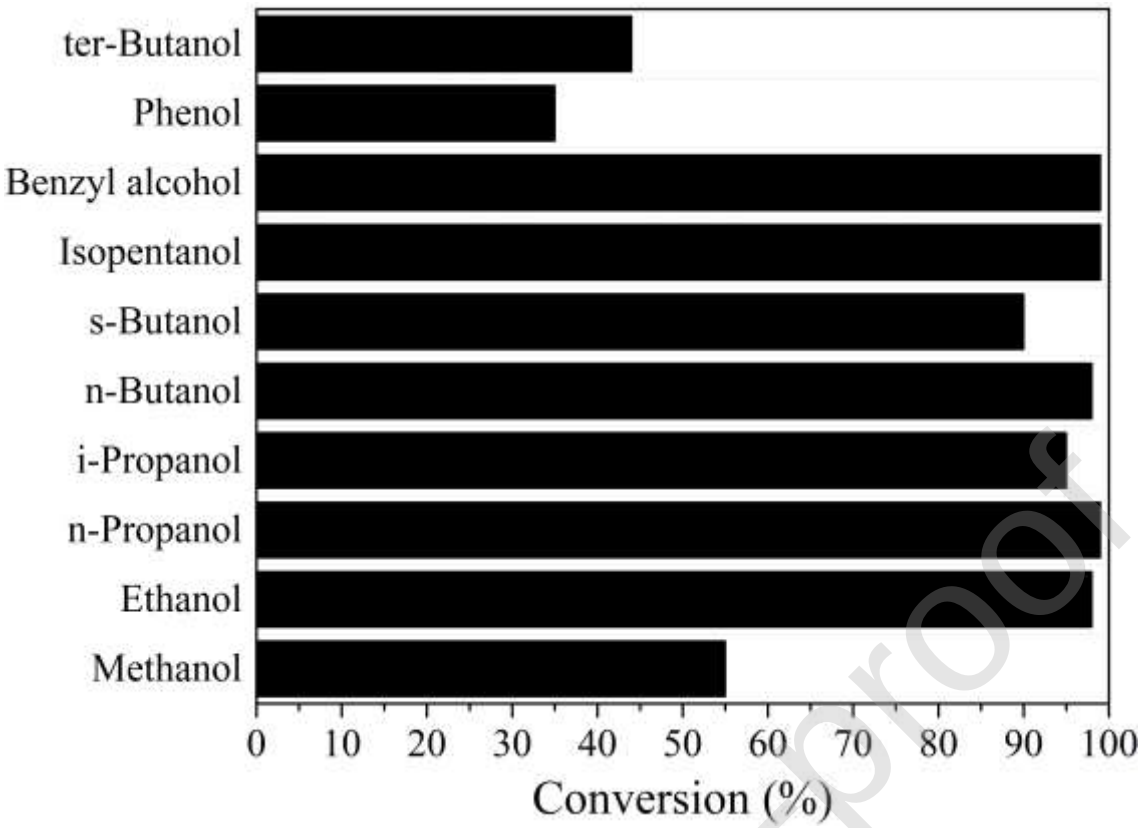


**Fig. 10.** Experimental (symbols), LH3 kinetic model (continuous lines) and ER3 kinetic model (dashed lines) for conversion profile of lauric acid at different catalyst amounts. Reaction conditions: 4 mmol lauric acid, 10 mL alcohol, $SiO_2$@20PMoV as catalyst, 58 °C.

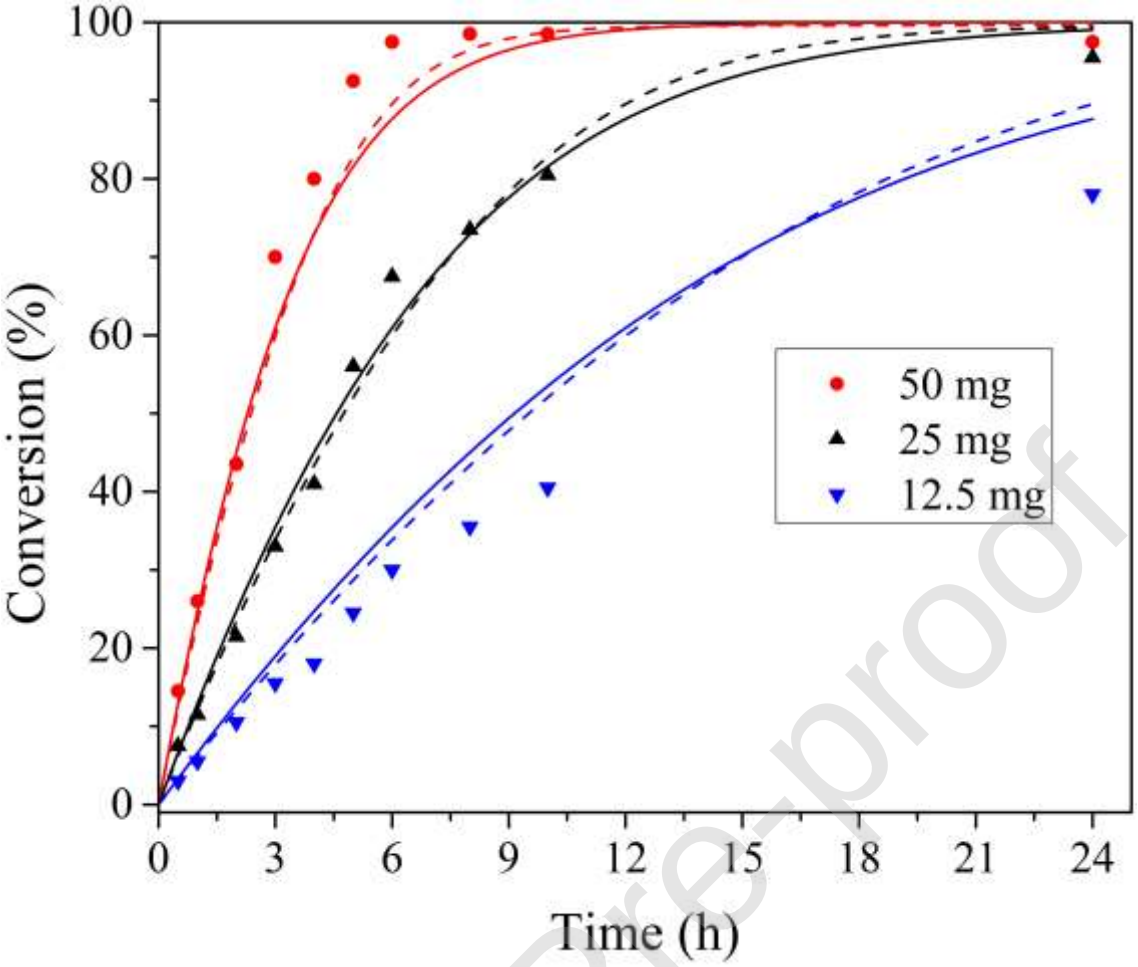


**Fig. 11.** Experimental (symbols), LH3 kinetic model (continuous lines) and ER3 kinetic model (dashed lines) for conversion profile of lauric acid at different ethanol amounts. Reaction conditions: 4 mmol lauric acid, 25 mg $SiO_2$@20PMoV, 58 °C.

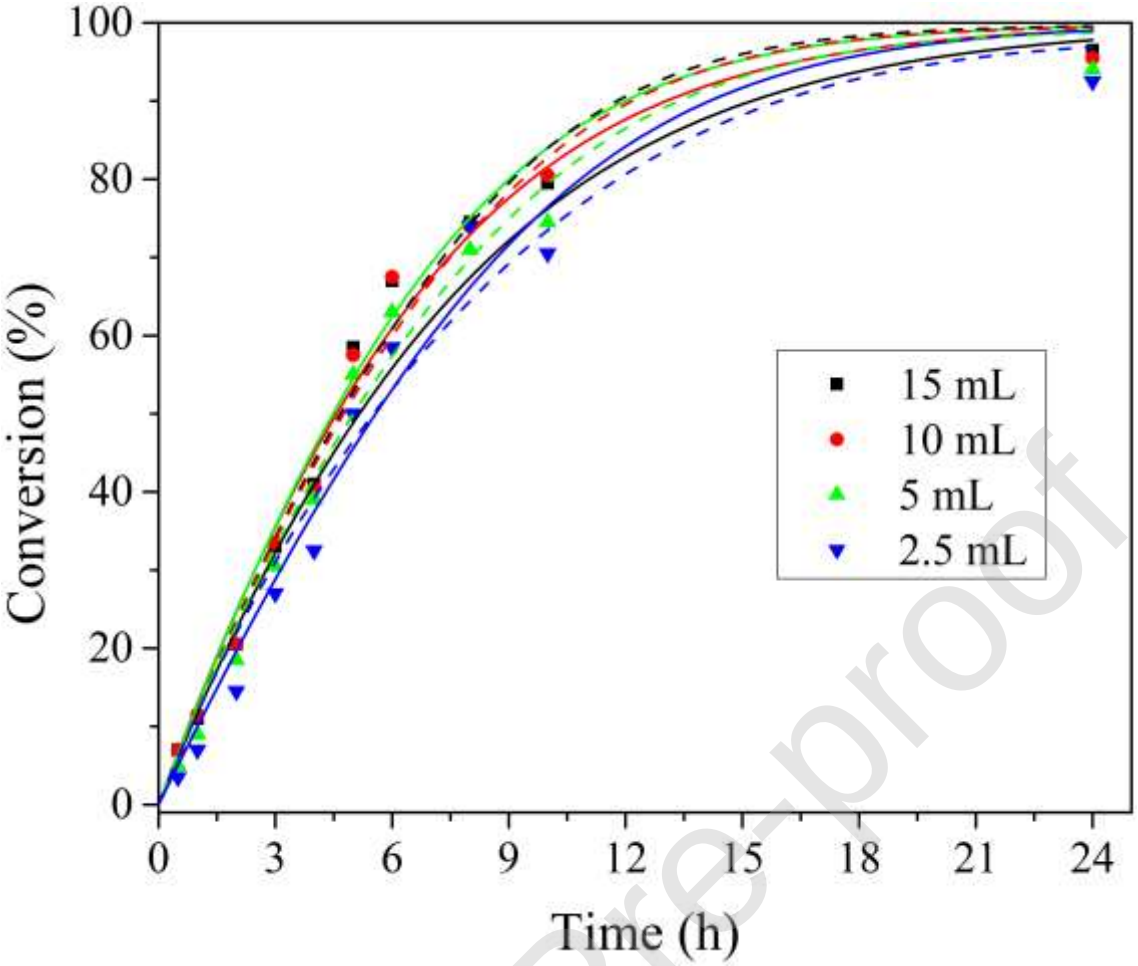


**Fig. 12.** Experimental (symbols), LH3 kinetic model (continuous lines) and ER3 kinetic model (dashed lines) for conversion profile of lauric acid at different temperatures. Reaction conditions: 4 mmol lauric acid, 10 mL alcohol, 25 mg $SiO_2$@20PMoV.

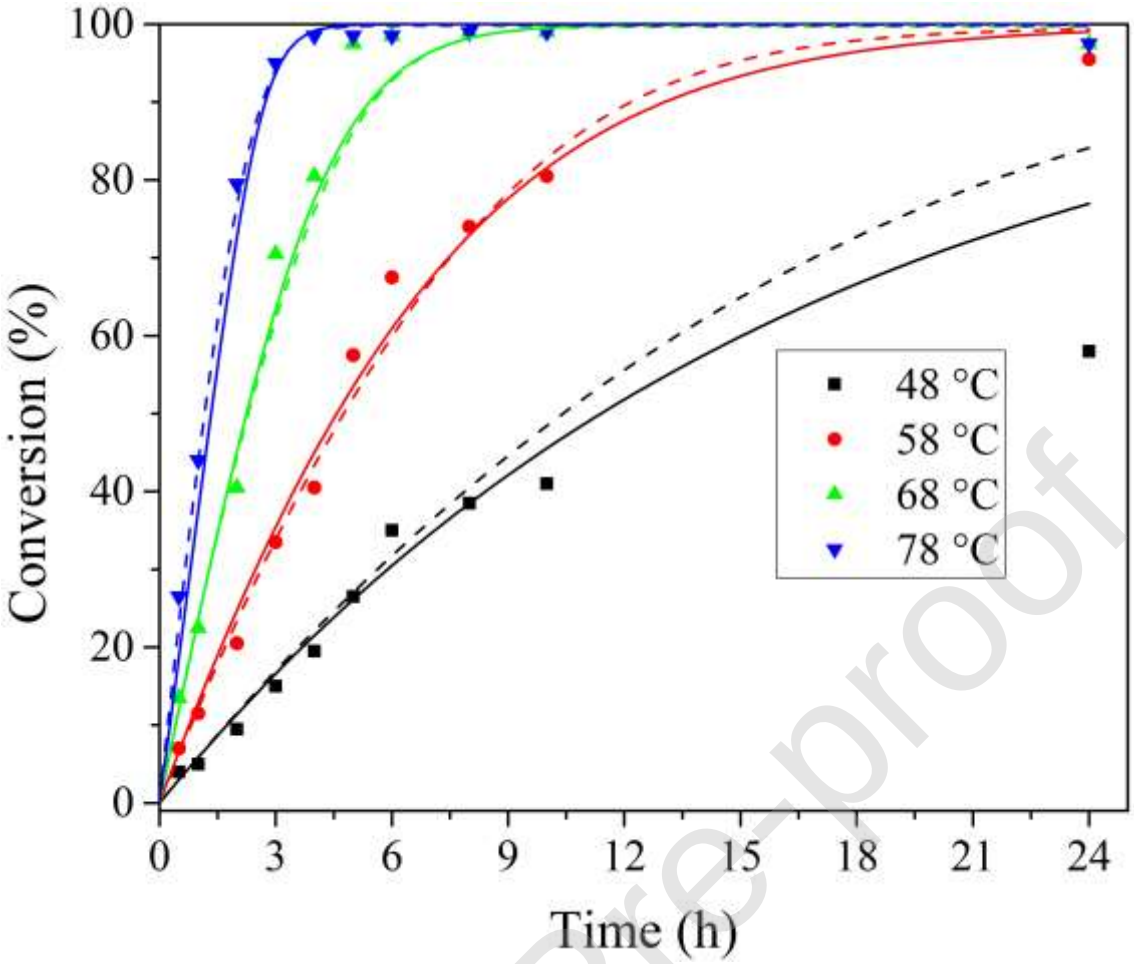


**Table 1.** Experimental conditions used for kinetic measurements of lauric acid esterification with ethanol, using $SiO_2$@20PMoV as catalyst.

| Run | T (°C) | Lauric acid (mmol) | Ethanol (mL) | Catalyst (mg) |
|---|---|---|---|---|
| 1 | 58 | 4 | 10 | 12.5 |
| 2 | 58 | 4 | 10 | 25 |
| 3 | 58 | 4 | 10 | 50 |
| 4 | 58 | 4 | 2.5 | 25 |
| 5 | 58 | 4 | 5 | 25 |
| 6 | 58 | 4 | 15 | 25 |
| 7 | 48 | 4 | 10 | 25 |
| 8 | 68 | 4 | 10 | 25 |
| 9 | 78 | 4 | 10 | 25 |

**Table 2.** Langmuir-Hinshelwood-Hougen-Watson (LHHW) kinetic models proposed for esterification reaction of lauric acid with ethanol.

| Model | Rate-limiting step<br>Definition of k | Rate equation (r) |
|---|---|---|
| LH1 | Acid lauric adsorption<br>$k = k_A C_t$ | $\frac{k\left[C_A - \frac{C_C C_D}{K_S K_A K_B K_C K_D C_B}\right]}{\left[1 + \frac{C_C C_D}{K_S K_B K_C K_D C_B} + K_B C_B + \frac{C_C}{K_C} + \frac{C_D}{K_D}\right]}$ |
| LH2 | Ethanol adsorption<br>$k = k_B C_t$ | $\frac{k\left[C_B - \frac{C_C C_D}{K_S K_A K_B K_C K_D C_A}\right]}{\left[1 + K_A C_A + \frac{C_C C_D}{K_S K_A K_C K_D C_A} + \frac{C_C}{K_C} + \frac{C_D}{K_D}\right]}$ |
| LH3 | Surface reaction<br>$k = k_S C_t^2$ | $\frac{k\left[K_A K_B C_A C_B - \frac{C_C C_D}{K_S K_C K_D}\right]}{\left[1 + K_A C_A + K_B C_B + \frac{C_C}{K_C} + \frac{C_D}{K_D}\right]^2}$ |

| | | |
|---|---|---|
| LH4 | Ethyl laurate desorption<br>$k = k_C C_t$ | $\frac{k\left[\frac{K_S K_A K_B K_D C_A C_B}{C_D} - \frac{C_C}{K_C}\right]}{\left[1 + K_A C_A + K_B C_B + \frac{K_S K_A K_B K_D C_A C_B}{C_D} + \frac{C_D}{K_D}\right]}$ |
| LH5 | Water desorption<br>$k = k_D C_t$ | $\frac{k\left[\frac{K_S K_A K_B K_C C_A C_B}{C_C} - \frac{C_D}{K_D}\right]}{\left[1 + K_A C_A + K_B C_B + \frac{C_C}{K_C} + \frac{K_S K_A K_B K_C C_A C_B}{C_C}\right]}$ |

**Table 3.** Eley-Rideal (ER) kinetic models proposed for esterification reaction of lauric acid with ethanol.

| Model | Adsorbed reactant | Desorbed product | Rate-limiting step<br>Definition of k | Rate equation (r) |
|---|---|---|---|---|
| ER1 | Lauric acid | Ethyl laurate | Adsorption<br>$k = k_A C_t$ | $\frac{k\left[C_A - \frac{C_C C_D}{K_S K_A K_C C_B}\right]}{\left[1 + \frac{C_C C_D}{K_S K_C C_B} + \frac{C_C}{K_C}\right]}$ |
| ER2 | | | Surface reaction<br>$k = k_S C_t$ | $\frac{k\left[K_A C_A C_B - \frac{C_C C_D}{K_S K_C}\right]}{\left[1 + K_A C_A + \frac{C_C}{K_C}\right]}$ |
| ER3 | | | Desorption<br>$k = k_C C_t$ | $\frac{k\left[\frac{K_S K_A C_A C_B}{C_D} - \frac{C_C}{K_C}\right]}{\left[1 + K_A C_A + \frac{K_S K_A C_A C_B}{C_D}\right]}$ |
| ER4 | Lauric acid | Water | Adsorption<br>$k = k_A C_t$ | $\frac{k\left[C_A - \frac{C_C C_D}{K_S K_A K_D C_B}\right]}{\left[1 + \frac{C_C C_D}{K_S K_D C_B} + \frac{C_D}{K_D}\right]}$ |
| ER5 | | | Surface reaction<br>$k = k_S C_t$ | $\frac{k\left[K_A C_A C_B - \frac{C_C C_D}{K_S K_D}\right]}{\left[1 + K_A C_A + \frac{C_D}{K_D}\right]}$ |
| ER6 | | | Desorption<br>$k = k_D C_t$ | $\frac{k\left[\frac{K_S K_A C_A C_B}{C_C} - \frac{C_D}{K_D}\right]}{\left[1 + K_A C_A + \frac{K_S K_A C_A C_B}{C_C}\right]}$ |

| | | | | |
|---|---|---|---|---|
| ER7 | Ethanol | Ethyl laurate | Adsorption $k = k_B C_t$ | $\frac{k\left[C_B - \frac{C_C C_D}{K_S K_B K_C C_A}\right]}{\left[1 + \frac{C_C C_D}{K_S K_C C_A} + \frac{C_C}{K_C}\right]}$ |
| ER8 | | | Surface reaction $k = k_S C_t$ | $\frac{k\left[K_B C_A C_B - \frac{C_C C_D}{K_S K_C}\right]}{\left[1 + K_B C_B + \frac{C_C}{K_C}\right]}$ |
| ER9 | | | Desorption $k = k_C C_t$ | $\frac{k\left[\frac{K_S K_B C_A C_B}{C_D} - \frac{C_C}{K_C}\right]}{\left[1 + K_B C_B + \frac{K_S K_B C_A C_B}{C_D}\right]}$ |
| ER10 | Ethanol | Water | Adsorption $k = k_B C_t$ | $\frac{k\left[C_B - \frac{C_C C_D}{K_S K_B K_D C_A}\right]}{\left[1 + \frac{C_C C_D}{K_S K_D C_A} + \frac{C_D}{K_D}\right]}$ |
| ER11 | | | Surface reaction $k = k_S C_t$ | $\frac{k\left[K_B C_A C_B - \frac{C_C C_D}{K_S K_D}\right]}{\left[1 + K_B C_B + \frac{C_D}{K_D}\right]}$ |
| ER12 | | | Desorption $k = k_D C_t$ | $\frac{k\left[\frac{K_S K_B C_A C_B}{C_C} - \frac{C_D}{K_D}\right]}{\left[1 + K_B C_B + \frac{K_S K_B C_A C_B}{C_C}\right]}$ |

**Table 4**. Textural porperties and acidity of catalysts.

| **Sample** | **$S_{BET}$ ($m^2/g$)** | **Pore Volume ($cm^3/g$)** | **Pore size (Å)** | **$E_0$ (mV)** |
|---|---|---|---|---|
| $SiO_2$ | 440 | 0.20 | 18.6 | 33.2 |
| $SiO_2$@5PMoV | 370 | 0.17 | 18.8 | 80.0 |
| $SiO_2$@10PMoV | 290 | 0.14 | 18.7 | 279.3 |
| $SiO_2$@15PMoV | 495 | 0.24 | 19.4 | 413.1 |

| | | | | |
|---|---|---|---|---|
| $SiO_2$@20PMoV | 545 | 0.27 | 20.0 | 433.3 |
| PMoV | - | - | - | 831.0 |

**Table 5.** Kinetic parameters for the pseudo-homogeneous model of esterification reaction of lauric acid with ethanol.

| **Parameter** | **Value** |
|---|---|
| $A_1$ ($L^{3.71}$/g.h.$mol^{2.71}$) | 124000 |
| $A_2$ ($L^{2.96}$/g.h.$mol^{1.96}$) | 113000 |
| $E_1$ (kJ $mol^{-1}$) | 60 |
| $E_2$ (kJ $mol^{-1}$) | 110 |
| α | 1.04 |

| | |
|---|---|
| β | 2.67 |
| γ | 1.48 |
| δ | 1.48 |
| **$R^2$ (%)** | 85.79 |



**Table 6.** Activation energies for the esterification reaction of lauric acid and ethanol catalyzed by different catalysts with pseudo-homogeneous model.

| Catalyst | $E_{a,\ direct}$ (kJ $mol^{-1}$) | $E_{a,\ reverse}$ (kJ $mol^{-1}$) | Reference |
|---|---|---|---|
| $SiO_2$@20PMoV | 60.00 | 110.00 | This study |
| $ZnL_2$ | 67.96 | 64.31 | [36] |
| [(*n*-bu-$SO_3H$)MIM][$HSO_4$] | 51.40 | | [37] |
| CTAB-DES | 48.78 | 40.66 | [38] |
| [Hnmp]$HSO_4$[a] | 68.45 | | [39] |

[a] methanol instead of ethanol.

**Table 7.** Kinetic parameters for the LHHW and ER kinetic models of esterification reaction of lauric acid with ethanol.

| Model | Parameter | | | | | | | | | |
|---|---|---|---|---|---|---|---|---|---|---|
| | **A (L $g^{-1}$ $h^{-1}$)** | **Ea (kJ $mol^{-1}$)** | **$K_A$ (L $mol^{-1}$)** | **$K_B$ (L $mol^{-1}$)** | **$K_C$ (mol $L^{-1}$)** | **$K_D$ (mol $L^{-1}$)** | **$K_S$** | **$R^2$** | **RMSE** | **NRMSE** |
| LH1 | 7.779E+04 | 37.966 | 1.270E+04 | 1.148E-04 | 4.095E+00 | 4.095E+00 | 4.846E+00 | 0.788 | 0.127 | 0.129 |
| LH2 | 5.003E+05 | 54.677 | 1.522E-06 | 6.040E+03 | 3.022E+02 | 9.472E+01 | 2.165E+01 | 0.943 | 0.066 | 0.067 |
| LH3[a] | 6.123E+07 | 56.337 | 2.988E+05 | 7.490E+03 | 1.241E+03 | 1.150E-05 | 5.211E+05 | 0.947 | 0.065 | 0.065 |
| LH4[a] | 2.748E+05 | 45.376 | 1.454E+01 | 3.260E+06 | 7.042E+07 | 1.789E-05 | 1.180E+04 | 0.914 | 0.081 | 0.082 |
| LH5[a] | 2.748E+05 | 45.376 | 1.454E+01 | 3.260E+06 | 1.789E-05 | 7.042E+07 | 1.180E+04 | 0.914 | 0.081 | 0.082 |
| ER1 | 2.361E+10 | 73.608 | 3.720E+07 | - | 9.170E+07 | - | 5.559E+07 | 0.757 | 0.136 | 0.137 |
| ER2 | 6.949E+05 | 55.357 | 4.320E+01 | - | 1.156E-01 | - | 1.567E-01 | 0.949 | 0.062 | 0.063 |
| ER3[a] | 3.378E+08 | 64.954 | 7.014E-01 | - | 2.442E+08 | - | 2.729E-01 | 0.960 | 0.055 | 0.056 |
| ER4 | 2.361E+10 | 73.608 | 3.720E+07 | - | - | 9.170E+07 | 5.559E+07 | 0.757 | 0.136 | 0.137 |
| ER5 | 6.949E+05 | 55.357 | 4.320E+01 | - | - | 1.156E-01 | 1.567E-01 | 0.949 | 0.062 | 0.063 |
| ER6[a] | 3.378E+08 | 64.954 | 7.014E-01 | - | - | 2.442E+08 | 2.729E-01 | 0.960 | 0.055 | 0.056 |
| ER7 | 1.000E+06 | 56.636 | - | 1.008E+07 | 3.586E+05 | - | 2.792E-06 | 0.947 | 0.064 | 0.064 |
| ER8 | 2.427E+07 | 52.239 | - | 1.301E-01 | 8.824E-02 | - | 7.259E+03 | 0.824 | 0.116 | 0.117 |
| ER9[a] | 4.334E+07 | 59.343 | - | 5.779E+07 | 6.475E+07 | - | 2.858E+00 | 0.950 | 0.062 | 0.063 |
| ER10 | 1.000E+06 | 56.636 | - | 1.008E+07 | - | 3.586E+05 | 2.792E-06 | 0.947 | 0.064 | 0.064 |
| ER11 | 2.427E+07 | 52.239 | - | 1.301E-01 | - | 8.824E-02 | 7.259E+03 | 0.824 | 0.116 | 0.117 |
| ER12[a] | 4.334E+07 | 59.343 | - | 5.779E+07 | - | 6.475E+07 | 2.858E+00 | 0.950 | 0.062 | 0.063 |

[a] Units of parameter A: mol $g^{-1}$ $h^{-1}$

**Table 8.** Kinetic parameters for the LH3 and ER3 models of esterification reaction of lauric acid with ethanol.

| Parameter | LH3 | ER3 |
|---|---|---|
| A (mol $g^{-1}$ $h^{-1}$) | 6.123E+07 | 3.378E+08 |
| $A_A$ (L/mol) | 2.997E+04 | 1.349E+00 |
| $A_B$ (L/mol) | 3.523E-06 | - |
| $A_C$ (mol/L) | 5.183E+03 | 1.828E+04 |
| $A_D$ (mol/L) | 3.450E+04 | - |
| $A_S$ | 5.176E+03 | 9.137E+02 |
| Ea (kJ $mol^{-1}$) | 56.072 | 64.824 |
| $\Delta H°_A$ (kJ $mol^{-1}$) | -5.996 | -0.019 |
| $\Delta H°_B$ (kJ $mol^{-1}$) | -59.354 | - |
| $\Delta H°_C$ (kJ $mol^{-1}$) | 31.750 | 17.150 |
| $\Delta H°_D$ (kJ $mol^{-1}$) | 61.332 | - |
| $\Delta H°_S$ (kJ $mol^{-1}$) | 15.071 | 24.531 |
| $R^2$ | 0.967 | 0.967 |
| RMSE | 0.051 | 0.050 |
| NRMSE | 0.051 | 0.050 |